FIU | Engineering & Computing

Department of Biomedical Engineering

GRADUATE RESEARCH DAY

SPRING 2024

DISCOVER | DESIGN | DEVELOP | DELIVER

GRADUATE RESEARCH DAY — Friday, March 8, 2024

The Biomedical Engineering Graduate Research Day showcases all the exciting research that our Biomedical Engineering graduate students are involved in. On Graduate Research Day, student researchers get the stage. It is a day-long opportunity for graduate students to gain valuable professional development experience, network with industry partners, present research, and learn about the research of others.

FIU | Engineering & Computing

Department of Biomedical Engineering

13th Annual

Graduate Research Day

Friday, March 8, 2024

Room EC 2300

7:30 am
Breakfast

8:45 am – 9:00 am
Welcome Remarks and Snacks

9:00 am – 10:15 am
Seminar with Dr. Delia Cabrera DeBuc, Research Associate Professor of Ophthalmology, University of Miami

10:15 am – 10:30 am
Short Break

10:30 am – 11:30 am
Oral Presentations

Panther Pit

11:30 am – 2:00 pm
Lunch & BMME Graduate Poster Session

Room EC 2300

2:00 pm – 3:15 pm
Oral Presentations 2

3:20 pm – 4:30 pm
Ethics Seminar with Dr. Andrew Brightman, Professor of Engineering Practice, Purdue University

4:30 pm – 5:00 pm
Awards Ceremony

MESSAGE FROM THE CHAIR

Today we celebrate your achievements. You serve as the backbone of our Department, and you continue to push us to new heights. We are proud of your hard work and dedication in advancing human knowledge and developing technologies that will transform the future of medicine. Research involves pushing the limits of our collective understanding, which requires inquisitiveness, resiliency, creativity, innovation, and intelligence.

The work that you present today demonstrates that you have the necessary attributes to conduct research at the highest level. The Graduate Research Day provides an opportunity to reflect on your accomplishments and showcase your work with pride.

As you move forward in your graduate education, continue motivating yourself and others around you to enhance your knowledge, remain inquisitive, and continue to grow in all aspects of learning.

Thank you to all who have worked to make this Graduate Research Day a success!

Best wishes for continued success,

Jorge Riera Diaz, Ph.D.

Interim Chair of Biomedical Engineering

KEYNOTE SPEAKER

EXPLORING BIOPHOTONICS FOR OCULAR AND BRAIN DISEASE DIAGNOSTIC

ABSTRACT: Advancements in Biophotonics offer promising avenues for diagnosing ocular and brain diseases through non-invasive and high-resolution imaging techniques. This interdisciplinary field integrates cutting-edge optical technologies such as optical coherence tomography (OCT), scanning laser ophthalmoscopy (SLO), laser speckle contrast imaging (LSCI), and functional near-infrared spectroscopy (fNIRS) to delve into the pathophysiology of neurodegenerative conditions. By leveraging these tools, researchers aim to identify novel biomarkers associated with diseases like diabetic retinopathy, multiple sclerosis, Alzheimer's, and Parkinson's. Their research aims to uncover distinctive structural and functional signatures indicative of disease onset, progression, and severity through rigorous investigation and analysis of optical imaging data. Insights gleaned from these studies hold significant implications for early diagnosis, prognosis, and therapeutic interventions for ocular and brain disorders. This investigation underscores the critical role of Biophotonics in advancing our understanding of neurodegenerative diseases and highlights the potential impact of optical imaging modalities in clinical practice and translational research.

Dr. Delia Cabrera DeBuc

Research Associate Professor of Ophthalmology, University of Miami

SHORT BIO: Dr. Delia DeBuc earned her Ph.D. in Applied Physics from the University of Michigan in 2002 and currently serves as a Research Associate Professor of Ophthalmology at the Bascom Palmer Eye Institute, University of Miami School of Medicine. With specialized training in ocular imaging technology and image analysis, she is renowned as a leading biophysicist in her field.

Dr. DeBuc's research group has garnered significant support from prestigious institutions, including grants from the Juvenile Diabetes Research Foundation, the National Institutes of Health, the Alzheimer's Association, the National Institute on Aging, the Finker Frenkel Legacy Foundation, and the National Eye Institute. Her research endeavors focus on advancing medical applications of ultrafast technology and optical imaging, particularly enhancing ocular healthcare capabilities. Dedicated to exploring novel ocular multimodal biomarkers in neurodegenerative eye and central nervous system diseases, such as diabetic retinopathy and Alzheimer's, Dr. DeBuc is at the forefront of groundbreaking research. She is deeply committed to leveraging Artificial Intelligence applications for disease diagnosis and runs a multidisciplinary lab that collaborates extensively with national and international investigators.

Using a multifaceted approach, Dr. DeBuc harnesses the power of AI/ML, XR applications, digital health, and brain-computer interfaces to investigate the intricate connections between the eye and the brain. Her efforts aim to unravel the relationship between neuronal pathways in the brain and the eye, ultimately advancing early disease detection methods. Dr. DeBuc's impactful contributions extend beyond her research endeavors. She is a Fulbright Scholar (2023-2024), the Guest Editor of the Special Issue "Ocular Biomarkers" Collection in Scientific Reports, and the co-founder of iScreen 2 Prevent LLC (DBA Multinostics), a spinoff from the University of Miami. With over 200 publications to her name, Dr. DeBuc's scholarly output has amassed over 4000 citations, reflecting her significant influence in the field (h-index: 33, i10-index: 61; Google Scholar)."

ETHICS SEMINAR

"BEYOND RESPONSIBLE CONDUCT OF RESEARCH TO DISCIPLINE-SPECIFIC ETHICS TRAINING: INSIGHTS FROM RESEARCH ON ETHICS ISSUES IN BIOMEDICAL ENGINEERING RESEARCH"

PRESENTED BY

Dr. Andrew Brightman

Professor of Engineering Practice,
Purdue University

ORAL PRESENTATIONS

Innovative Markers and Techniques for Heart Failure Detection

Authors: Valentina Dargam and Joshua Hutcheson

Faculty Advisor: Dr. Joshua Hutcheson

Despite recent advancements in surgical interventions and pharmacotherapies used to treat heart failure (HF), HF outcomes remain poor and hospitalizations continues to rise. Early diagnosis and management of the conditions that cause HF could prevent adverse cardiac remodeling and irreversible functional impairment that lead to poor patient outcomes. The goal of this study is to identify new markers of cardiac remodeling and develop advanced techniques to analyze cardiac signals to detect early HF.

We use two different mouse models to study the progression of heart failure and associated biomarkers. Mice were fed special dietary regimens to induce either chronic kidney disease (CKD) with cardiac dysfunction or HF with preserved ejection fraction (HFpEF). We assessed changes in cardiac structure and function via echocardiography, electrocardiography, phonocardiography, cardiac catheterization, plasma biomarkers, and histology.

Preliminary results show that early markers of HF can be detected noninvasively prior to functional changes. Mice in the CKD and HFpEF regimens had significantly higher right-ventricular pressure as early as week 3 when compared to control mice (Fig. 1A). Our electrocardiogram data showed that the duration of Speak-p markers was also significantly higher than controls at week 6 of the CKD diet. In the HFpEF model, higher right-ventricular pressure was observed at week 3, prior to echocardiogram-based functional changes. So far, our results show the potential of using new, noninvasive biomarkers to detect early signs of HF.

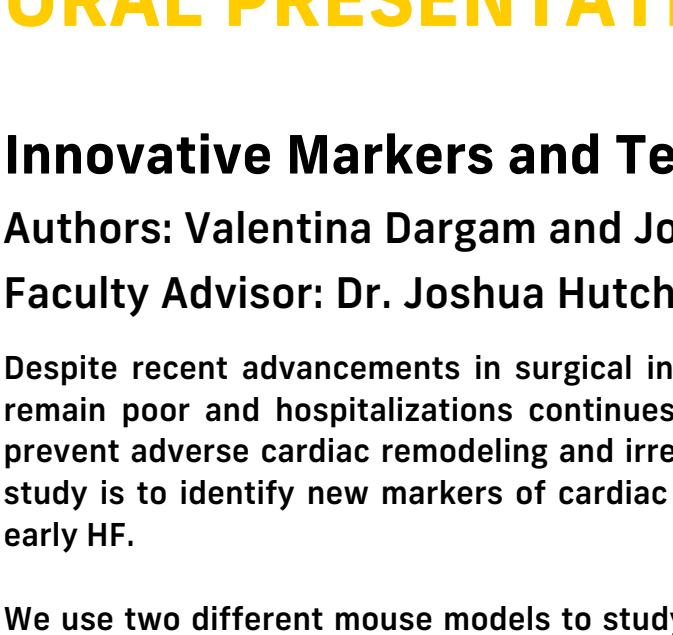

Fig. 1: A) Right-ventricular pressure measured invasively via cardiac catheterization. Duration of **B)** second heart sound (S2) and **C)** Sp-p electrocardiogram maker throughout disease progression.

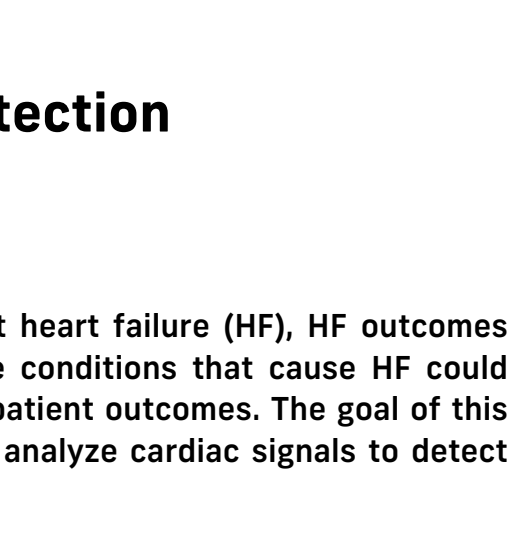

Immunofluidic platform for multiple biomarker detection to identify stages of coronary artery disease and heart failure

Authors: Lin Tong and Joshua Hutcheson

Faculty Advisor: Dr. Joshua Hutcheson

Coronary artery disease (CAD) is the most common type of cardiovascular disease (CVD) and most CVD ends with heart failure (HF). The direct medical costs of CVD are approximately $1 billion per day, most of which is spent on treatment rather than prevention, even though most cardiac disease is preventable. Prevention is an important aspect of reducing the burden of CVD and includes education, exercise, diet, and lifestyle management. However, individuals often do not strictly adhere to prevention guidelines unless there are clear signs of risk. Therefore, risk assessment and early diagnosis are crucial to help inform patients and drive lifestyle changes. Meanwhile, an early intervention and management of HF can also improve the quality of life, but we lack the evaluation tools for HF management. Underserved communities have limited access to health care, which results in health disparities, including cardiovascular disease. Thus, our goal is to develop a low-cost, easy-to-use, point-of-care immunofluidic platform for multiple biomarker detection to identify stages of coronary artery disease and heart failure. We accomplish this by (1) combining established cardiac biomarkers, including cardiac Troponin I (cTnI), N-terminal propeptide BNP (NT-proBNP), high-sensitivity c-reactive protein (hs-CRP) and an emerging biomarker, sortilin, to predict risk of cardiac disease in a pre-clinical model and (2) developing a polydimethylsiloxane (PDMS) based immunofluidic point-of-care device for multi-biomarker panel (Figure 1) with a novel calibration mesh (Figure 2) for a wide clinical detection range.

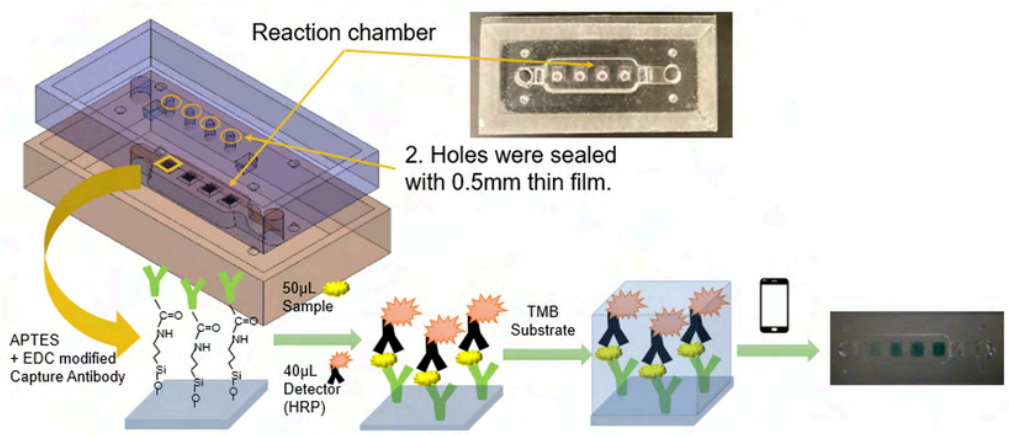

Fig. 1 Schematic of immunofluidic platform.

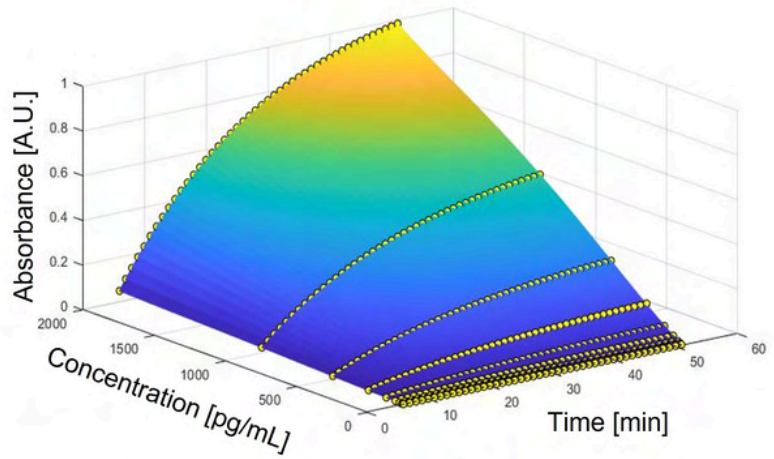

Fig. 2 Cardiac Troponin I calibration mesh.

Characterizing Astrocyte-Mediated Neurovascular Coupling by Combining Optogenetics and Biophysical Modeling

Authors: Alejandro Suarez and Jorge Riera

Faculty Advisor: Dr. Jorge Riera

Astrocyte-mediated Neurovascular Coupling comprises several biomechanical pathways by which resource delivery to neural tissue is regionally regulated. These pathways have been actively charted in past decades proving astrocytic calcium activity to be the common signaling trigger. However, there is still a lot of controversy about each pathway's contribution to the hemodynamic response. We hypothesize that they enact a vascular response in a dynamic, non-linear fashion. To evaluate our hypothesis, we utilized a tetracycline-based double transgenic mouse model which allows optogenetically stimulation exclusively to cortical astrocytes. Localized changes in cerebral blood flow (CBF) were measured via Laser Doppler Flowmetry (LDF) modality. Stimulated regions demonstrated a sustained increase in localized CBF. Subsequent pharmacological inhibition of Group IIA secreted phospholipase A2 (sPLA2), Group IV cytosolic PLA2 (cPLA2), and voltage-gated potassium (BK) channels facilitated the characterization of all proposed biochemical pathways. Sole inhibition of sPLA2 or BK channels induced oscillatory behavior in the CBF baseline following drug application implying their contribution towards maintaining vascular tone. Lastly, we developed a computational biophysical model of the hemodynamic response encompassing all known calcium-triggered mechanisms of SMC contractility and validated it using our experimental data. We conclude that astrocytic-mediated NVC mechanisms are nonlinear and non-additive, and that separating them might require integrated approaches based on biophysical modeling and experimental designs.

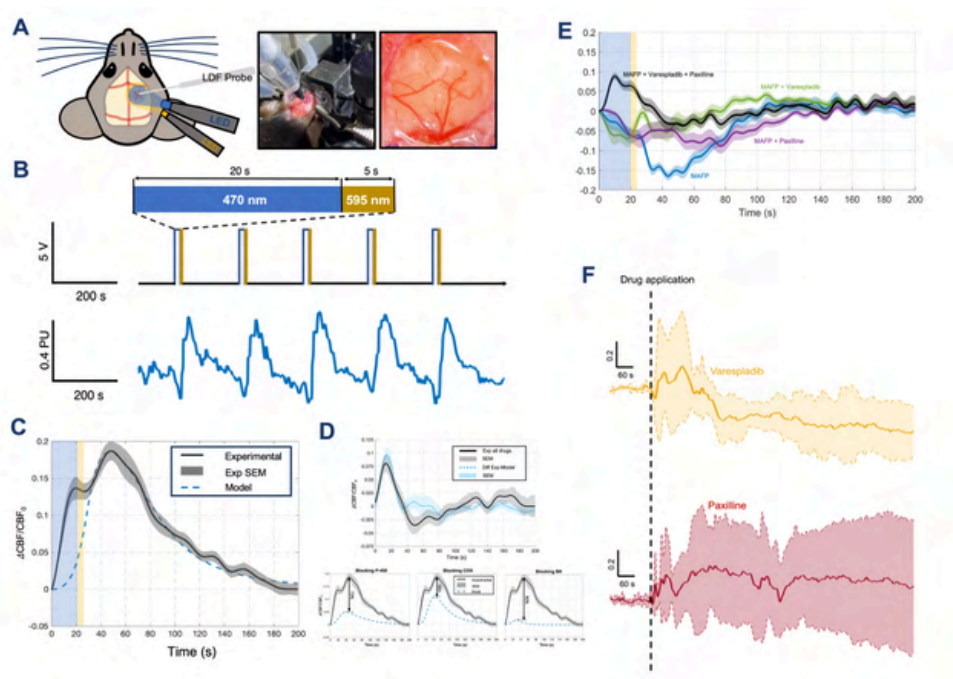

Fig. 1 A) Experimental design. *Left panel*: Cartoon of the mouse craniotomy showing LDF probe and LEDs placement. Major pial vessels were avoided when positioning the LDF probe. *Right Panel*: Real pictures of the experimental setup and craniotomy. **B) Stimulation paradigm**. *Right top panel*: Blue bar denotes the duration (20 s), wavelength (470 nm) and power (3 mW) of the blue LED; Yellow bar denotes the denotes the duration (5 s), wavelength (595 nm) and power (0.5 mW) of the amber LED. *Middle panel*: Stimulation paradigm used for each experimental condition studied. *Bottom panel:* Pre-processed LDF data (CBF) (lowpass filtered 0.5 Hz). **C) Experimental vs theoretical CBF response in normal conditions (vasodilation).** Black line - Relative change in localized blood flow in ChR2-Mlc1 mice (n=5); it shows a sustained increase in CBF. Gray shadow - standard error of the mean (SEM). Dashed blue line - Modeled response using parameter optimization of the theoretical model. **D) Model compliance to experimental data.** Top panel: Dark gray line – experimental CBF response after the application of all drugs; light blue dotted line – difference between the experimental CBF response without drugs and the fitted theoretical CBF response shown in Figure 3B - left panel. Bottom panel: Theoretical response after blocking the main signaling pathways (left – P450, center – COX, right - BK). CBF response decreased by ~73% after blocking P-450 enzyme; ~38% after blocking COX enzyme; and ~90% after blocking BK channels. **E) Relative changes in CBF in response to stimulation for 4 different combinations of drugs:** *Blue:* MAFP; *Green:* MAFP + Varespladib; *Marron:* MAFP + Paxilline; *Black:* MAFP + Varespladib + Paxilline. **F) Unstable behavior in CBF after drug application.** Relative changes in CBF right after the application of application (*Top panel* - Varespladib; *Bottom Panel*- Paxilline) show unstable oscillations of the response.

The effect of coronary ostium height on asymmetric onset of aortic valve calcification in a chronic kidney disease mouse model of calcific aortic valve disease

Authors: Daniel Chaparro and Joshua Hutcheson

Faculty Advisor: Dr. Joshua Hutcheson

Aortic valve (AoV) calcification is a condition where bone-like mineral deposits form on the AoV. These deposits render the valve dysfunctional and if left untreated can lead to heart failure and death. Variations in the hemodynamic environment of valvular tissues can increase the calcification potential of the tissue. Areas of high shear tend to have lower amounts of calcification while areas of low or disturbed shear tend to have more calcification. In one of our previous studies, we show that mice on a high adenine high phosphate diet develop AoV calcification in an asymmetric manner. In these mice, the right coronary cusp (RCC) is more calcified than the left. These mice also have high take off right coronary ostia (RCO) which would have an impact on the hemodynamic shear experienced by the RCC. In this study we aim to determine the effect of RCO height on RCC calcification. We hypothesize that a higher RCO origination will induce lower shear stresses and higher calcification burden on the RCC. Computational fluid dynamics of shear stresses on the AoV reveal that there is a significant drop off of wall shear stress during diastolic loading on the RCC when the RCO originates above the sinotubular junction (Figure 1). From our mouse studies, we show that there is a positive correlation between RCO origination height and RCC calcification but a negative correlation between RCO origination height and KLF2 expression (Figure 2). This suggests that hemodynamic shear differences between the aortic valve cusps due to coronary orifice origination heights may play a significant role in the asymmetry in calcification burden seen in calcific aortic valve disease (CAVD).

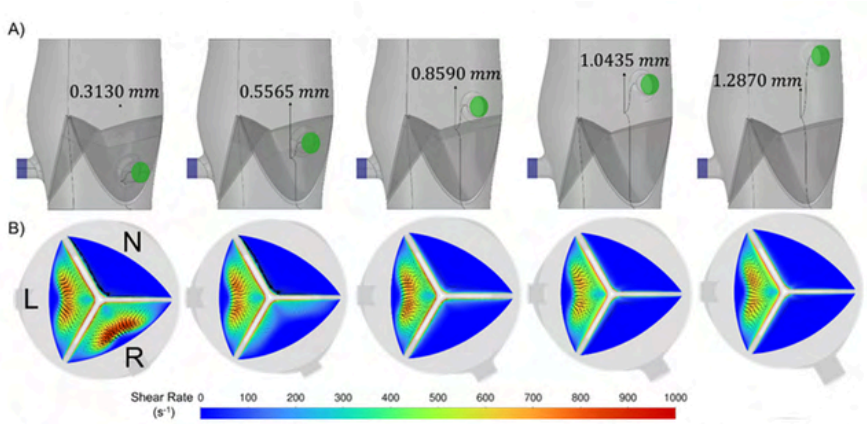

Fig. 1 Computational fluid dynamics simulation of shear rate on the aortic surface of aortic valve leaflets as the right coronary ostium origination height is increased.

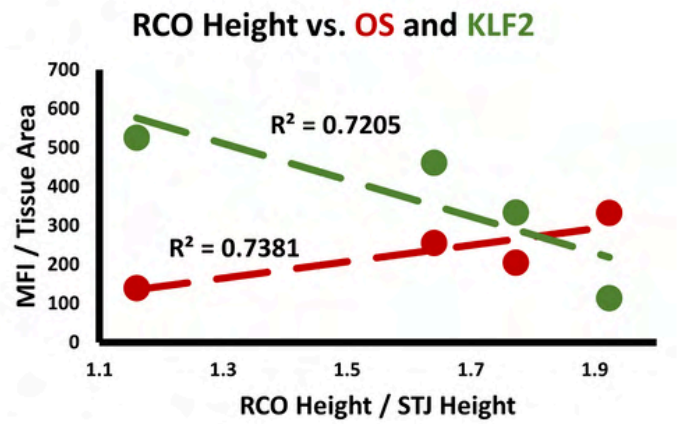

Fig. 2 Correlation between right coronary ostium height and calcification as quantified by OsteoSense signal (RED). Correlation between right coronary ostium height and KLF2 immunofluorescence expression (GREEN).

Fluid-Structure-Interaction Models of Early-Stage Calcified Aortic Valves Show Hemodynamics Biomarkers

Authors: Asad Mirza and Sharan Ramaswamy

Faculty Advisor: Dr. Sharan Ramaswamy

Diagnosis of calcific aortic valve disease (CAVD), the most prevalent human adult heart valve disorder, is generally done after symptoms present themselves. Indeed, before diagnosis, hydrodynamic quantities, such as pressure gradient (ΔP), mean flow rate (QRMS), effective orifice area (E.O.A), and regurgitant fraction (RF), are often indistinguishable from a healthy valve. Our goal was to identify if there existed hemodynamic biomarkers, such as time-averaged wall shear stress (TAWSS), attained through fluid-structure (FSI) simulations of blood and tissue of a bioengineered valve, that present at early-stage CAVD even if there were no changes in hydrodynamics.

Porcine small intestinal submucosa (PSIS) bio-scaffold valves (N=9) were seeded with valvular interstitial/endothelial cells (VICs/VECs). They were then equally cultivated under a calcifying media with either static or high oscillatory flow, compared to a raw PSIS control group. Hydrodynamic and nanoindentation assessment was done to record pressure, flow, and tissue stiffness per valve. Valve and surrounding geometry were modeled in SolidWorks 2022 and meshed using ANSYS LS-PREPOST. FSI simulations were then conducted using a strong coupling algorithm in ANSYS LS-DYNA.

Hydrodynamic assessments showed parameters were below thresholds associated for even mild calcification. Young's modulus, however, was 73.25 kPa in cultured valves versus 55.10 kPa control. FSI simulations of these valves agreed within 30% of hydrodynamic assessment and showed an increase in WSS between calcified and raw groups (Fig. 1). Indeed, TAWSS was 18.96 dynes/cm2 in calcified groups and 12.41 dynes/cm2 in raw valves.

This study demonstrates that following changes in hemodynamics, such as TAWSS, might be a numerical metric for diagnosing early-stage valve calcification, facilitating patient monitoring through clinical imaging and computational modeling.

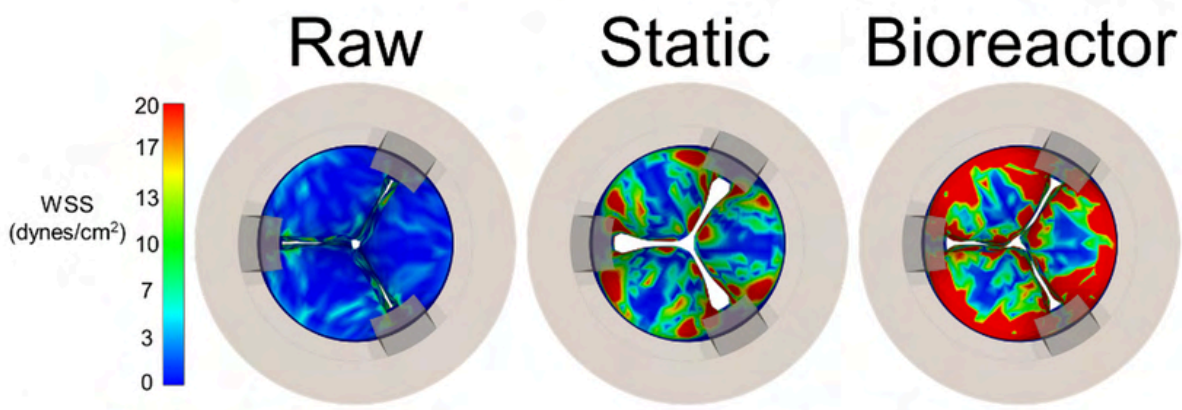

Figure 1. WSS maps of fibrosa surface during peak diastole between raw, static, and bioreactor conditioned groups.

Multiscale electrical signatures of interneuron in agranular frontal cortex of macaques during performance monitoring

Authors: Beatriz Herrera and Jorge Riera

Faculty Advisor: Dr. Jorge Riera

Extracellular potentials have been assumed to originate mainly from the postsynaptic potentials and nonlinear dendritic dynamics of pyramidal cells (PCs). Thus, most biophysical modeling studies have focused on evaluating the local field potentials (LFPs), current source density (CSD), and EEG signatures of distinct PC populations in different cortical areas. Only a few studies have examined the contribution of GABAergic interneurons to these signals. Yet, they have primarily focused on basket cells and considered a limited number of interneurons and morphology reconstructions. Furthermore, they did not account for differences in the interneurons laminar across cortical areas nor considered external inputs associated with experimental paradigms. Here, we evaluated the contribution of GABAergic interneurons in the agranular frontal cortex to the extracellular potentials, considering their actual density throughout the cortical laminae and a total of 54 detailed biophysical models with distinct morphological reconstructions. We found that CB and PV populations have a nonnegligible contribution to the LFP/CSD and EEG, while the CR interneurons only contribute to the signal as white noise (Figure 1A). Furthermore, we examined the combined contribution of error PCs and SEF interneurons to the ERN and Pe-component (Figure 1B). Our results suggest that the combined activity of error PCs and interneurons more closely resembled the SEF CSD-derived EEG. Our work reports, for the first time to our knowledge, a nonnegligible contribution of interneuron populations to extracellular potentials.

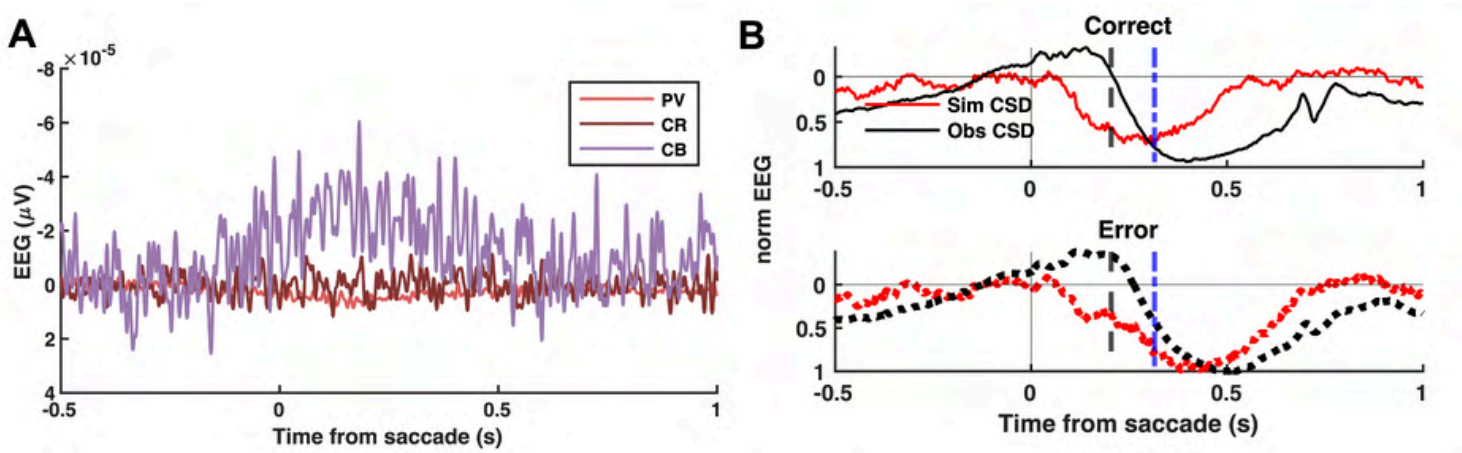

Figure 1: SEF interneurons contribution to the EEG. **A.** EEG evoked by the activity of SEF interneurons (PV – parvalbumin, CB – calbindin, and CR – calretinin). **B.** Comparison of SEF-CSD EEG (black – Obs CSD) and simulated-CSD EEG (red – Sim CSD) for correct (top) and error (bottom) trials. The amplitude of the EEG signals was normalized by the maximum absolute EEG amplitude across trial types for Obs CSD EEG and Sim CSD EEG separately. The time of peak polarization of ERN (dash) and Pe (dot–dash) are indicated.

Precision Medicine with Radioactive Iodine for Thyroid Cancer: A novel and robust method to quickly estimate and report thyroid remnant dose

Authors: Xiang Kong and Anthony McGoron

Faculty Advisor: Dr. Anthony McGoron

The thyroid gland is highly avid for iodine. Radioiodine (RAI) is commonly used to ablate thyroid small remnants remaining after total thyroidectomy surgery, as it can selectively destroy any remaining thyroid cells. However, current guidelines are still based on empirical evidence and there remains controversy surrounding the optimal dosage.

Targeted radionuclide therapy dosimetry can be approached through two different methods: the mean absorbed dose and voxel-based dosimetry. Mean absorbed dose (D) approach has been the common method historically. D = A * Δ, where A is the total cumulated activity, and Δ is the equilibrium dose constant. The main challenges include accurately estimating the true activity and target mass. In recent years substantial progress has been made in the computation of absorbed dose at the voxel level. A voxel S-value represents the mean absorbed dose to a target voxel per radioactive decay in a source voxel. Standardized uptake value (SUV) is a widely used parameter in clinical PET imaging. When conducting a I-124 PET imaging study, SUVmax is more meaningful because it reflects the local maximum concentration of radioactive iodine within the lesion, which in turn corresponds to the maximum dose.

Six patients were successfully enrolled in our IRB-approved clinical trial. 13 thyroid remnants were identified through PET/CT. Both the mean absorbed dose and SUVmax dose were calculated for each remnant. A comprehensive analysis of the normalized mean activity and SUVmax curve reveals a clear correlation between these parameters. Statistical analysis is performed between the mean absorbed dose and maximum lesion dose. Remarkably, the results demonstrate a strong correlation between the mean absorbed dose and SUVmax dose. This validation underscores the reliability of the relationship between these two metrics. Such findings provide valuable insights into a quick and robust estimation of absorbed dose, contributing to improved patient care in RAI therapy.

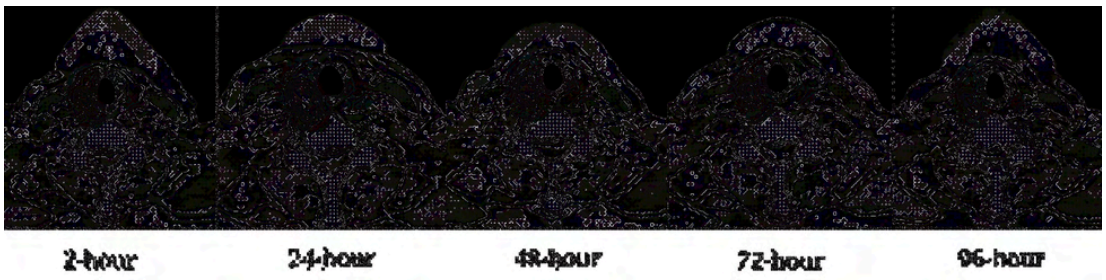

Fig 1. A series of 3D PET/CT images from a patient used for dose calculation.

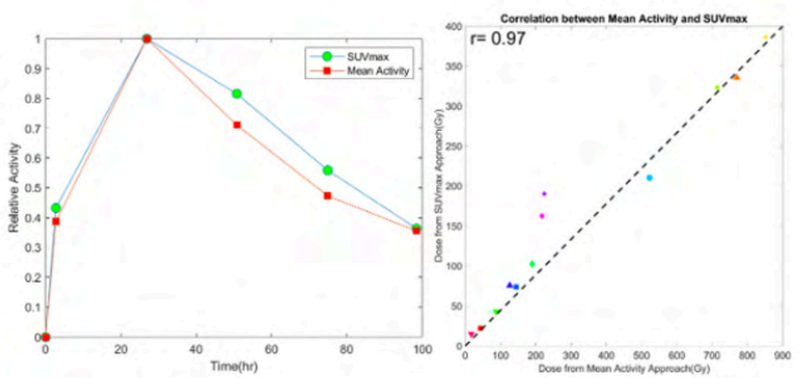

Fig 2. A strong correlation is shown between the mean activity and SUVmax *method.*

POSTER PRESENTATIONS

Dynamic Phantom for PPG signal validation with skin tone and obesity variation

Authors: Tananant Boonya-ananta and Jessica Ramella-Roman

Faculty Advisor: Dr. Jessica Ramella-Roman

Cardiovascular disease is one of the leading cause of death in the US. Current blood pressure systems are intrusive and non-continuous. Optical wearable systems can provide continuous critical health information of the cardiac system. We aim to develop a dynamic pulsatile phantom that mimics optical, geometrical, and mechanical properties of the radial artery at the wrist to evaluate PPG signal with variations from skin tone and obesity levels in a diverse population. Design criteria meets optical, fluid and biomechanical properties at the wrist radial artery. Initial measurements shows realistic pulsatile index and maintains similar properties to real physiological parameters. PPG signal is recorded at different artieral depth simulation obesity and different optical properties with additional silicon phantom layer for different skin tones.

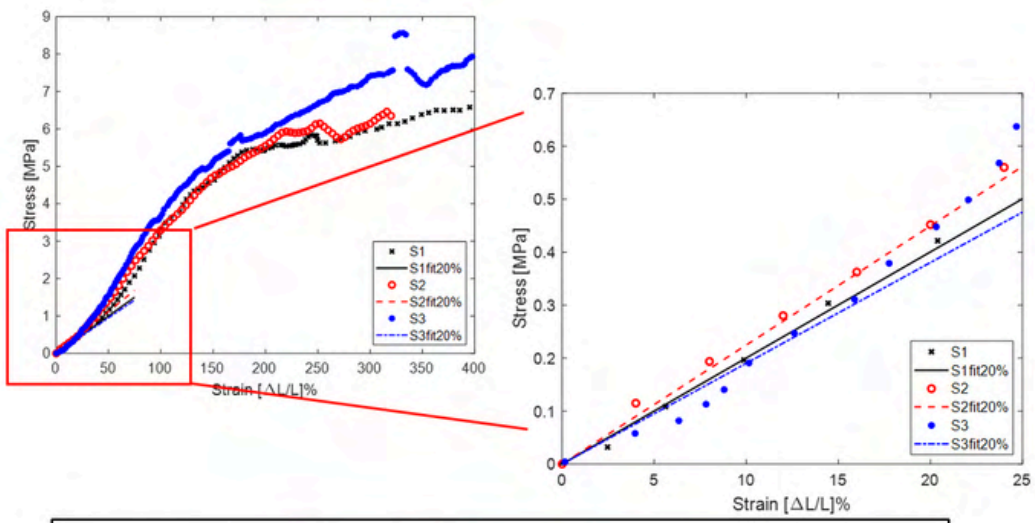

Figure 1. Mechanical properties measurement

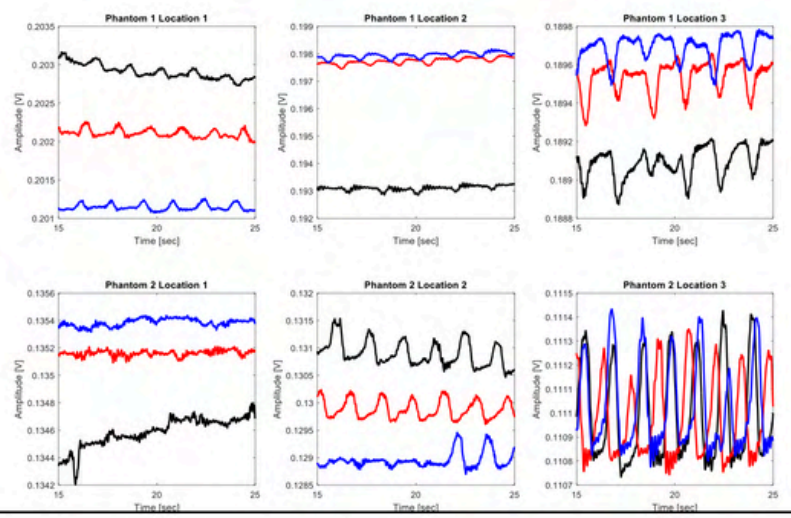

Figure 2. PPG signal with skin tone and depth

Depth-resolved Mueller Matrix analysis of cervical remodeling in pregnant mice

Authors: Ajmal, JunZhu Pei, and Jessica Ramella-Roman

Faculty Advisor: Dr. Jessica Ramella-Roman

Preterm birth remains a significant challenge in maternal and neonatal healthcare. The uterine cervix undergoes extensive remodeling during pregnancy to facilitate successful childbirth. The extracellular matrix (ECM) plays a pivotal role in this remodeling process, affecting cervical biomechanics and its ability to maintain structural integrity throughout gestation. However, early softening of the uterine cervix due to accelerated remodeling of the cervix ECM leads to Preterm Birth. In this study, we performed Mueller matrix polarization imaging of mice cervix at different pregnancy time points and analyzed polarization parameters to assess the associated cervical collagen remodeling. The polarization imaging was carried out using our independent polarimeter devised to provide transmission and reflected light Mueller Matrix microscopy images called the TRIMMM.

Our research focuses on the depth-resolved Mueller matrix polarization assessment of the ECM structure evolution of mice cervix sections, spanning from external OS to the internal OS of the cervical region, at different gestation stages. The Mueller matrix-derived polarization parameters efficiently map the tissue microstructure and composition of the mice cervix due to the optical anisotropy of the collagen fibers in the ECM. Our statistical analysis of the MM results yields valuable information on the variation in the micro-structural organization of the cervical ECM across depths at day 6, day 12, day 15, and day 18 of gestation periods in mice. These findings demonstrate the potential of polarization-sensitive imaging techniques for accurate and fast diagnosis of PTB risk in clinical settings and contribute to developing PTB risk prediction and targeted interventions.

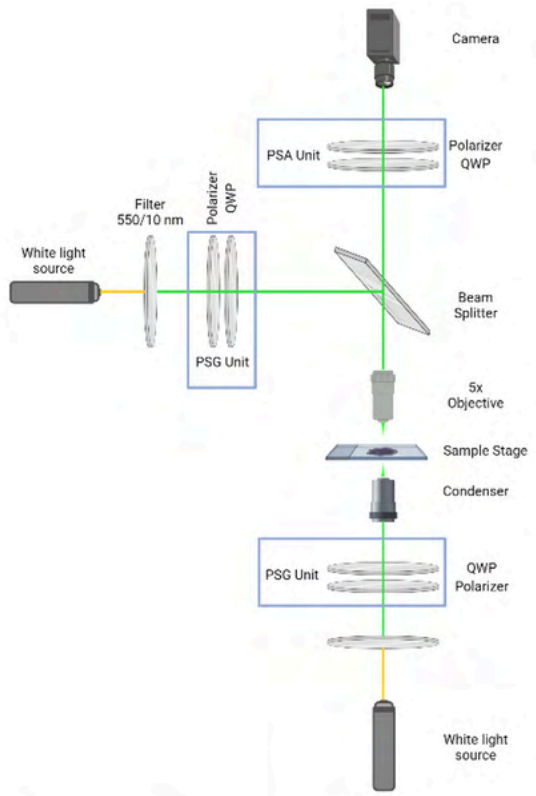

Fig. 1. Schematic of the experimental setup TRIMMM

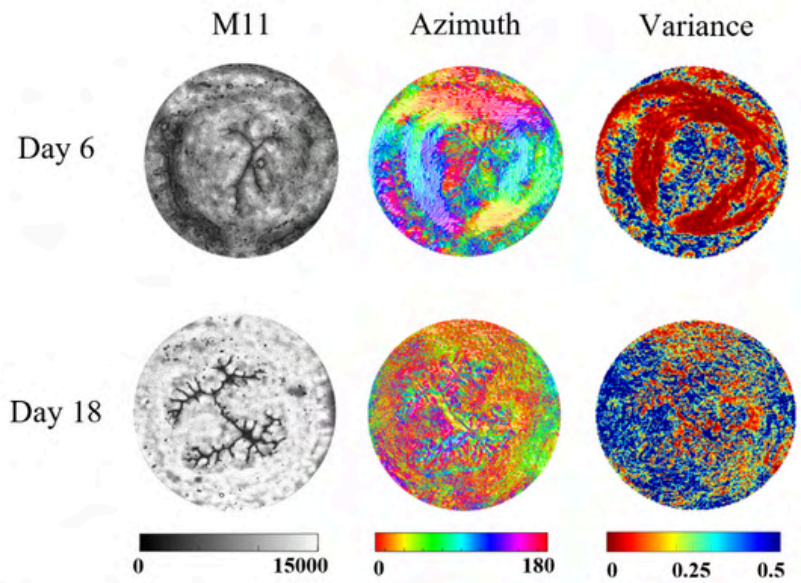

Fig. 2. Total reflectance image (M11), polarization azimuth of cervical tissue, and variance of cervix section at 200 μm depth from Day 6 and Day 18.

Changes in hemodynamic correlation maps in mice with vascular calcification

Authors: Aasma Dahal, Daniela Leizaola, Faiza Nazir, Valentina Dargam, Joshua Hutcheson, and Anuradha Godavarty

Faculty Advisors: Dr. Joshua Hutcheson and Dr. Anuradha Godavarty

Chronic kidney disease (CKD) increases the risk of vascular calcification (VC), a leading predictor of cardiovascular morbidity and mortality. Our previous study suggested hemodynamic changes in the peripheries were different with and without calcification during peripheral imaging of murine tails. However, these results were based on hemodynamic changes at point locations, and the overall changes in the entire peripheral tail were not determined. Our current work focuses on understanding the overall changes in hemodynamic correlation throughout the murine tail with and without VC. Here, ten-week-old adult mice were placed on a special diet for 12 weeks to induce CKD (CKD group) and CKD-induced VC (CKD group). Murine tails were imaged using an in-house near-infrared optical scanner (NIROS) and the spatiotemporal diffuse reflected NIR signals were obtained in response to occlusion. Occlusion-induced changes (during the first occlusion cycle) in hemoglobin-based parameters were obtained and analyzed to determine the hemodynamic correlation maps. The hemodynamic correlation maps based on effective oxy-(ΔHbO) and total-hemoglobin (ΔHbT) changes exhibited a predominantly negative correlation in the CKD+VC group compared to the CKD group at week 12 (n=5) (sample case shown in Fig 1). This suggests a disruption of flow patterns due to the presence of VC in the CKD+VC group compared to the CKD group. These observed changes may be due to calcification in altering vascular compliance and blood flow. Ongoing work will focus on a more thorough comparison across weeks.

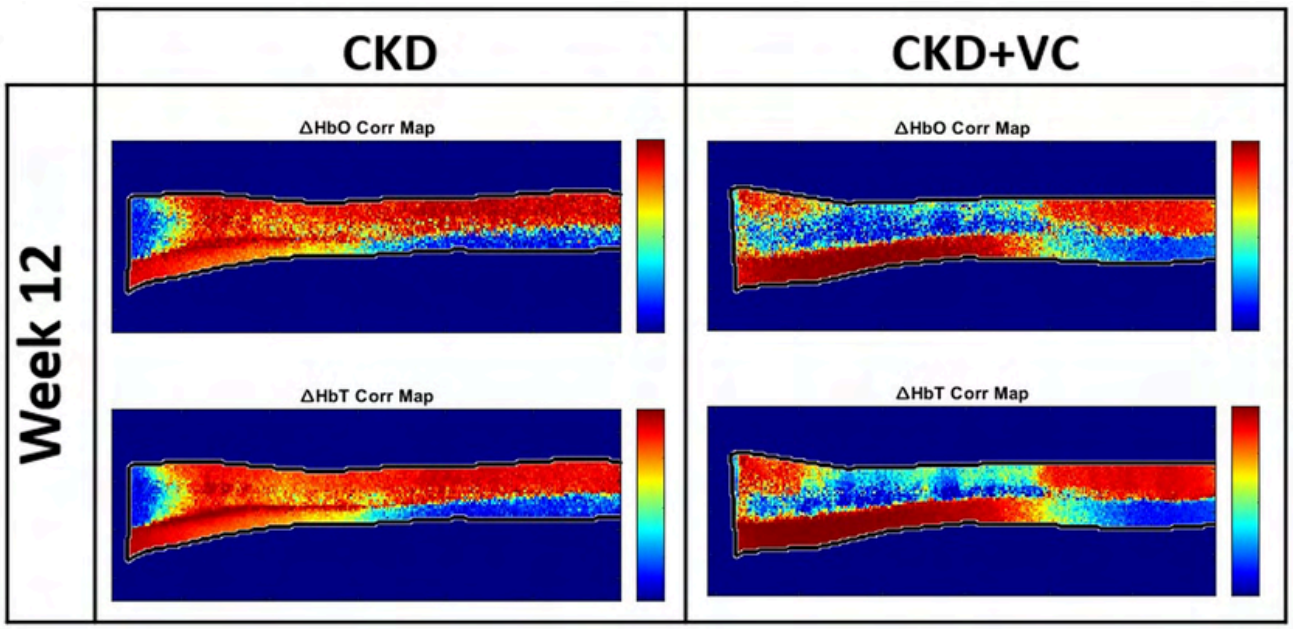

Fig 1: Pearson's based correlation map at week 12 for hemodynamic parameters ΔHbO, and ΔHbT for mice without and with vascular calcification(CKD and CKD+VC).

Implication of Primary vs Secondary Cell Wall of Plants Vascular Tissue in Designing Bioinspired Materials

Authors: Salman Jamal and Anamika Prasad

Faculty Advisor: Dr. Anamika Prasad

Vascular Cells wall plays a big role in structural and functional development of plants. The diversified role covers from the defense, support, growth to the conduction of nutrients and ions of plants. Such plant-based inspiration provides sufficient evidence as an engineering template to develop bioinspired biomaterials. The transition of plants from primary to secondary cell wall and its constituent components (cellulose, hemicellulose, pectin, and lignin) interplay a big role in active growth of plants while maintaining all the necessary function. In this experiment, we delve into understand the modification of Primary cell wall to secondary cell wall and due mechanical response in the cell wall architecture. The plant stalk samples were subjected to enzymatic treatment to evaluate the role of its constituents in plant cell wall by removing specific components and characterized at different stages of life using Raman spectroscopy and SEM imaging, and Nanoindentation. SEM images shows comparatively thick cell wall in the xylem region of the mature samples and confirms the selective modification due to enzymatic treatment, while Raman spectroscopy analyses the presence of carbohydrates bonds to represent the cellulosic and hemicellulose materials at the different stage of growth. The mechanical properties were evaluated using the Nanoindentation to find the elastic modulus and the hardness, a significant outcome of the experiment. Major findings suggests that the pectin and lignin have distinctive role in designing the cell wall, and the attenuated mechanical properties also get influenced with the dynamic molecular level changes of the constitutive components in cell wall.

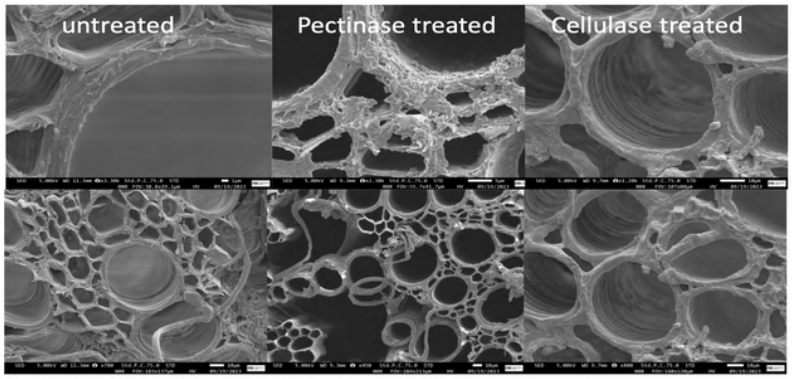

Figure. 1- SEM Images of Enzyme treated Cell Wall.

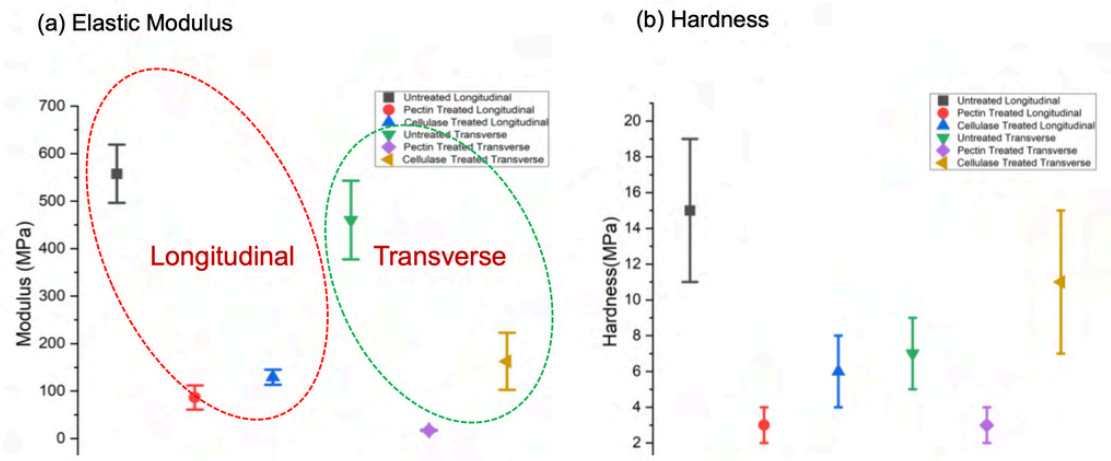

Fig. 2- Elastic Modulus and Hardness properties of Cell wall via Nanoindentation testing.

Multiscale Modeling of the Impacts of Arteriolar and Capillary-Driven Signaling on Brain Blood Flow Regulation

Authors: Dabasish Kumar Saha and Nikolaos Tsoukias

Faculty Advisors: Dr. Nikolaos Tsoukias

Neurovascular communication (NVC) is fundamental for maintaining regular brain function but can become compromised in brain disorders. Capillaries play a critical role in monitoring neuronal activity because of their proximity to neurons. Recent findings suggest that capillaries possess the ability to detect and initiate vasoactive signaling. Nonetheless, the coordination of blood flow distribution in the microvascular network through arteriolar and capillary mediated NVC remains unclear. The intricate structural nature and challenges of experimental observation necessitate modeling to gather insights into these mechanisms. In this investigation, we integrate cell-level models into a multicellular in-silico representation of capillaries and arterioles within a reconstructed microvascular network. Biomechanical models translate electrical and calcium signals into alterations in vessel diameter, thereby predicting network hemodynamics in macroscale tissue volumes. We conduct simulations to explore the impact of local stimulation by applying a hyperpolarizing K+ stimulation to an arteriole or capillary segment, inspecting electrical conduction along the network and resultant changes in blood flow distribution. At lower levels of stimulation, hyperpolarizing signal remains localized to the stimulated area, prompting a modest increase in local blood flow perfusion. Higher levels of stimulation are necessary for the vasodilatory signal to propagate over considerable distances and reach upstream feeding vessels. Furthermore, simulations examine the role of K+ as an NVC mediator in arterioles and/or capillaries. The dissemination of the electrical signal depends on Kir channel density, that plays dual role as a K+ sensor and an amplifier of propagating electrical signals. The model explores the biophysical determinants of capillary and arteriole-driven vasodilatory signaling and their impacts on brain blood flow regulation.

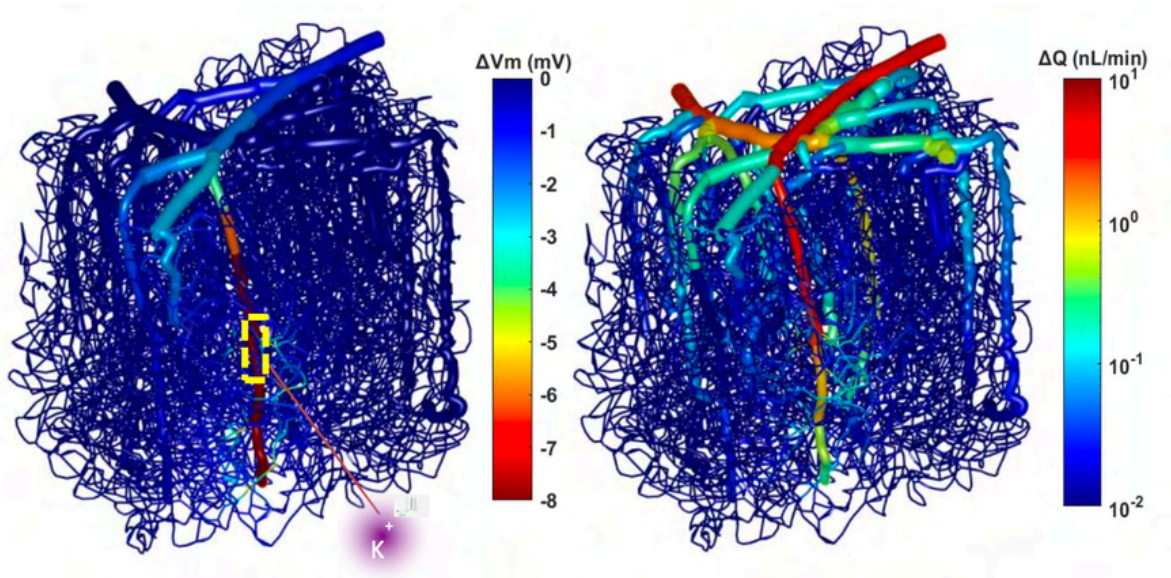

Alteration of V_m and Blood flow dynamics in a mouse cerebral microvascular network upon arteriolar stimulation.

Battery-less, Multichannel and Wireless Recorder for Neuronal Activity Monitoring in Swine

Authors: Melany Gutierrez-Hernandez, John Volakis, and Jorge Riera

Faculty Advisors: Dr. John Volakis and Dr. Jorge Riera

Our multidisciplinary group has been recognized for introducing and developing a battery-less, multichannel, wireless neurosensing system (mWiNS; Chen et al. 2018; Chen et al. 2019). The operation of this system is based on radiofrequency (RF) backscattering and optical communications for multiplexing capabilities. Benchtop and in vivo evaluation in rodents of the system has been performed in the past (Moncion et al. 2019, Moncion et al. 2022). However, we have not been able to fully implant the multichannel system in an animal in vivo because of the relatively large footprint size and the type of animal we have been using. This study addresses these issues by introducing two new approaches. First, the multichannel system is well packaged and miniaturized to 45x29mm2 footprint (Fig. 1), 60% less compared to our latest design that included multichannel operation (40x40mm2) and matching circuit (29x57mm2) for high impedane electrodes. Secondly, we introduce, for the first time, the use of a regulated large animal (swine) for a fully implantation. The system miniaturization was feasible by employing a multilayer design and 3D additive manufacturing technology with dielectric and conductive inks. In addition, we reduce by half the antenna size by introducing shorted pins. The communication link between the implant and interrogator antennas was also improved, demonstrating better performance over previous designs for different skin depth. Importantly, in this study we evaluate the capability of recording epileptic form like activity by monitoring somatosensory evoked potentials (SSEP) with fore and hind limb stimulations (Fig. 2). SSEP are of the same order of epileptic form discharges 50-300μV. This will create the foundation for evaluating the system in chronic epileptic pigs in the future.

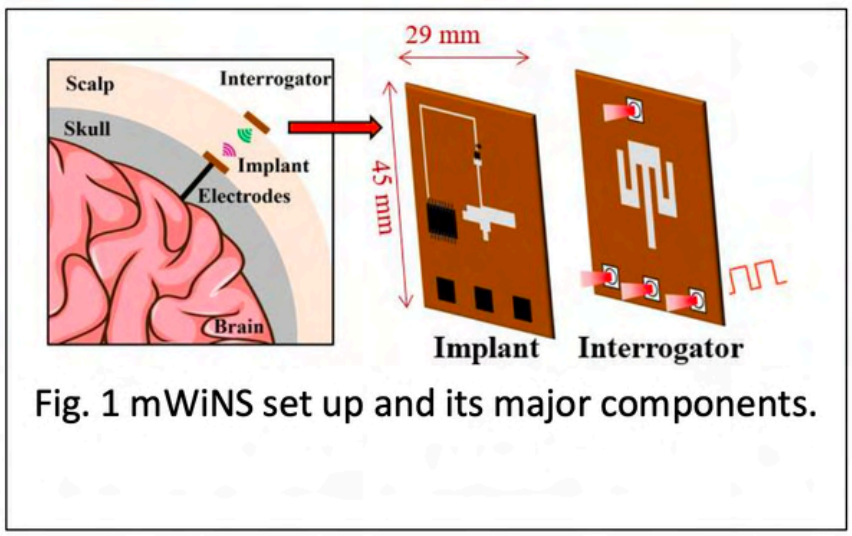

Fig. 1 mWiNS set up and its major components.

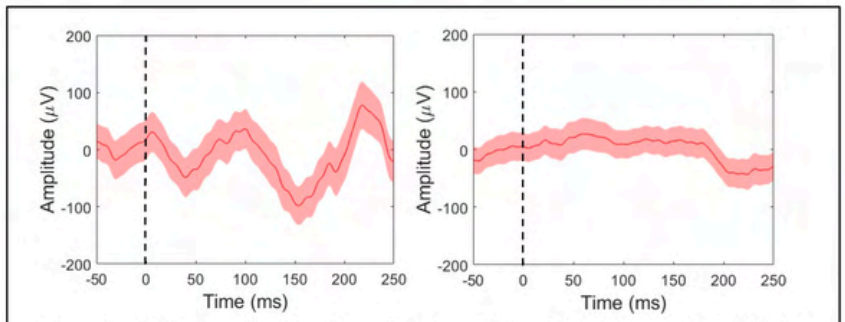

Fig. 2 SSEP of single channel activation (Left) in response to hind limb stimulation (dashed line) compared to the lack of response under the control, no stimulation (right).

Lipidomic and Proteomic Characterization of Calcifying Extracellular Vesicles

Authors: Katherine Kaiser, Lillian Valadares Tose, Francisco Fernandez-Lima, and Joshua Hutcheson

Faculty Advisor: Dr. Joshua Hutcheson

Vascular calcification is the most significant predictor of an individual's risk of heart attack. In response to pathological conditions, such as hypertension and mechanical stress, vascular smooth muscle cells (VSMCs) that line the artery wall transition to an osteoblast (HOB) like phenotype. This allows VSMCs to produce similar hydroxyapatite mineral that HOBs produce naturally, for the purpose of potentially stabilizing atherosclerotic plaques and resisting vascular deformation. In both forms of mineralization, cells release small membrane bound compartments called extracellular vesicles (EVs) that carry pro-calcific cargo into the extracellular space to nucleate mineral formation. Despite the similarity of these processes, recent data suggest that the mechanism through which VSMCs create calcifying EVs is distinct from that of HOBs. To further investigate this, our group will isolate EVs from VSMCs and HOBs grown in osteogenic media and identify their lipidomic and proteomic composition. We aim to use this profile of lipids and proteins to identify unique characteristics between the two EV populations, thus providing more insight into their individual mechanistic origins.

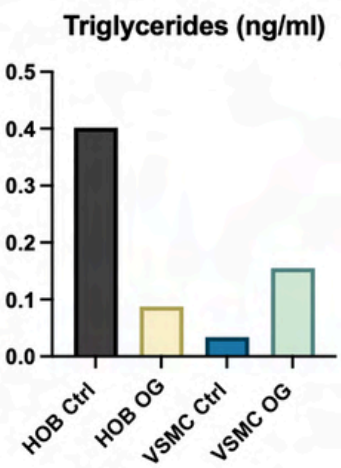

Fig. 1 Triglyceride content of extracellular vesicles released from human osteoblasts (HOB) and vascular smooth muscle cells (VSMC) in control or osteogenic conditions.

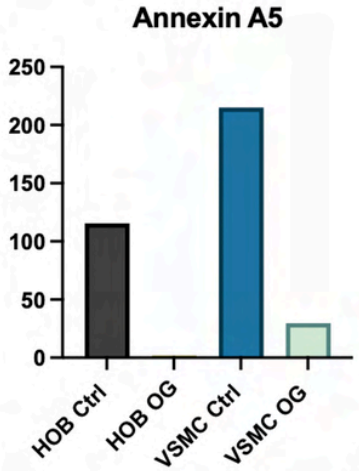

Fig.2 Annexin A5 protein content on extracellular vesicles released from human osteoblasts (HOB) and vascular smooth muscle cells (VSMC) in control or osteogenic conditions.

EGFR inhibition prevents CAV1-dependent calcifying extracellular vesicle biogenesis

Authors: Sophie Ashbrook and Joshua Hutcheson

Faculty Advisor: Dr. Joshua Hutcheson

Vascular calcification represents the most significant predictor of cardiovascular events with no current therapeutic options for prevention or treatment. Osteogenically-differentiated vascular smooth muscle cells (VSMCs) release calcifying extracellular vesicles (EVs), which nucleate nascent mineral. Caveolin-1 (CAV1), a plasma membrane scaffolding protein residing in caveolar domains, plays a critical role in the formation of calcifying EVs. Previous studies have reported interactions between CAV1 and epidermal growth factor receptor (EGFR) in cancer pathology. Given the nature of these reported interactions, we hypothesized that EGFR inhibition may prevent the biogenesis of calcifying EVs by altering CAV1 trafficking. We assessed the potential of EGFR tyrosine kinase inhibition (AG1478 and PD153035, 2.5 uM, N = 3) to prevent calcification in vitro using VSMCs cultured in osteogenic media (OS) for 28 days and in vivo (AG1478 and PD153035, 10 mg/kg, N = 40) using a chronic kidney disease (CKD) diet model to induce medial calcification. In vitro, EGFR inhibition significantly prevented the release of calcifying EVs in OS cultures ($p < 0.01$ and $p < 0.001$). In vivo, calcification was significantly decreased by EGFR inhibition ($p < 0.05$). The decrease in vascular calcification by EGFR appeared independent from effects on kidney function. EGFR inhibition also decreased the release of calcifying EVs when given after 14 days of OS treatment in vitro, a time point at which VSMCs have adopted a pro-calcific phenotype and continued for an additional 14 days ($p < 0.01$). Our results suggest that EGFR interferes with trafficking mechanisms that are required for calcifying EV biogenesis. EGFR inhibition effective at preventing calcification prior to pro-calcific stimuli in vitro and in vivo and following initiation of calcification in vitro. Future studies will test the efficiency of different EGFR inhibitors, both tyrosine kinase and ligand binding, at different concentrations, to determine the most effective therapeutic options. Given that EGFR inhibitors exhibit clinical safety, the current data show that EGFR may be a propitious target in preventing vascular calcification.

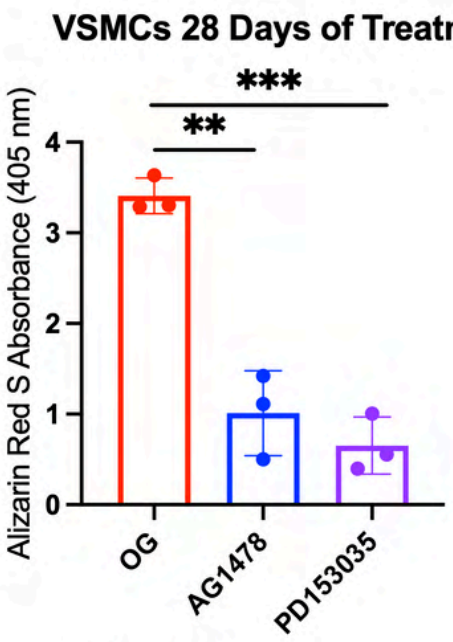

Fig. 1 **********

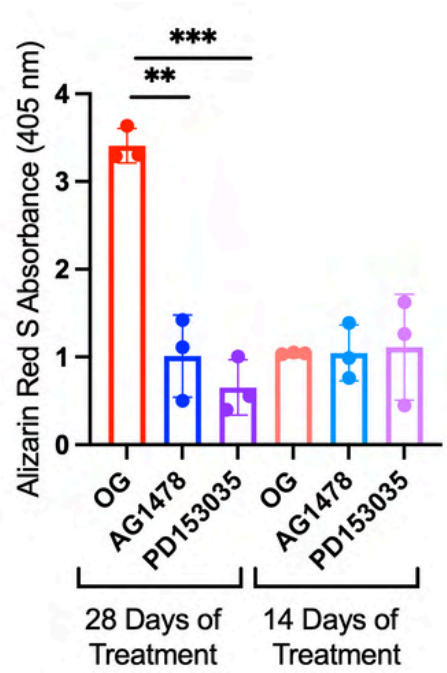

Fig. 2 **********

The Myogenic Regulation of Cerebral Blood Flow: A Mathematical Model for Electromechanical Coupling in Arteriolar Smooth Muscle and Capillary Pericytes

Authors: Niloufar Khakpour and Nikolaos Tsoukias

Faculty Advisor: Dr. Nikolaos Tsoukias

Capillary-mediated signaling has emerged as a significant component of neurovascular coupling (NVC), allowing blood perfusion to match local demands in the brain. Capillary Pericytes (PCs) can actively regulate capillary tone and diameter and respond to electrochemical signals or changes in pressure. In this study, we present an integrated modeling approach that can link macroscale flow responses to cell-level dynamics, and we explore the role of capillary PCs in coordinating local blood flow distribution and mediating NVC. The cell level models describe membrane potential (Vm) and Ca2+ dynamics in capillary endothelial cells (cECs) and pericytes (PCs), as well as in endothelial (ECs) and smooth muscle cells (SMCs) of parenchymal arterioles (PAs) and pial arteries (Fig. 1). Biomechanical models of arterioles and capillaries are employed to translate Ca2+ signals into changes in vessel diameter. The model is compared against experimental data capturing arteriolar and capillary responses to pressure or extracellular K+ challenges. Network level simulations show how myogenic autoregulation maintains a relatively constant brain perfusion as blood pressure increases. Interestingly, the model suggests significant contribution by contractile capillaries in addition to arterioles in this phenomenon. Simulations further explore the physiological relevance of PCs regulating capillary diameters, identifying two potentially critical regulatory roles. First, PC-mediated, capillary adaptation can promote more uniform blood flow distribution when arterioles constrict. This can preserve blood supply to the deeper and more vulnerable regions of the brain. Second, capillary-level myogenic autoregulation can promote "blood stealing" by redistributing perfusion from unstimulated brain regions towards regions of neuronal activity, maximizing resource utilization.

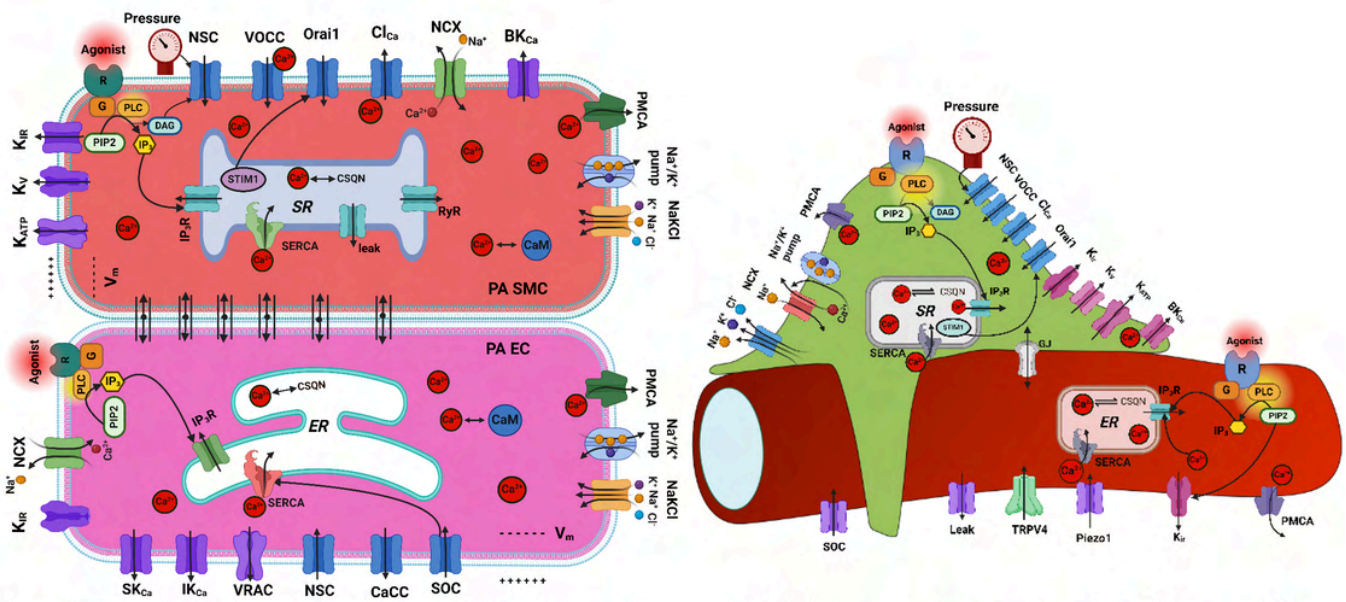

Fig. 1. Mathematical models of cell electrophysiology and Calcium dynamics are developed for capillary endothelial cells (cECs), Pericytes (PCs), and Parenchymal Arterioles (PA) ECs and SMCs.

Therapeutic effects of relaxin receptor agonists on *in vivo* and *in vitro* models of vascular calcification

Authors: Ana Valentín Cabrera, Courtney Myhr, Roxana Melo, Katelan Sugrim, Alexander Gonzalez, Kenneth Wilson, Juan Marugan, Joshua Hutcheson, and Alexander Agoulnik

Faculty Advisor: Dr. Joshua Hutcheson

Vascular calcification contributes to the rupture of atherosclerotic plaques—the leading cause of heart attacks. No therapeutics exist to treat vascular calcification. We suggested that relaxin, a vasoprotective and anti-fibrotic small peptide hormone of the insulin/relaxin family, may affect this condition. However, recombinant relaxin has short stability *in vivo*, poor bioavailability, and is expensive to synthesize, limiting its clinical utility for chronic conditions such as vascular calcification. As an alternative, ML290 is a biased allosteric agonist of the human relaxin receptor (hRXFP1) previously shown to attenuate vascular calcification in *Apoe-/-* mice. This study aimed to determine if ML290 may reverse arterial remodeling with lifestyle interventions and develop an *in vitro* assay to compare multiple relaxin agonists on alkaline phosphatase activity, a key enzyme in the development of vascular calcification. A high-fat diet-induced atherosclerosis and vascular calcification in humanized (hRXFP1/hRXFP1) *Apoe-/-* mice for 15 weeks. To simulate lifestyle changes, mice were returned to the chow diet for the last 10 weeks of the experiment. Mice were divided into four groups: vehicle with atherogenic diet, ML290 with atherogenic diet, vehicle with chow diet, and ML290 with chow diet. In addition, we developed an *in vitro* assay to compare multiple relaxin agonists on alkaline phosphatase activity in human aortic vascular smooth muscle cells (haVSMC). Preliminary data suggest that relaxin agonism reduces alkaline phosphatase activity dose-dependently in haVSMCs. This study demonstrates the potential to determine the most suitable small-molecule relaxin agonists for vascular calcification treatment.

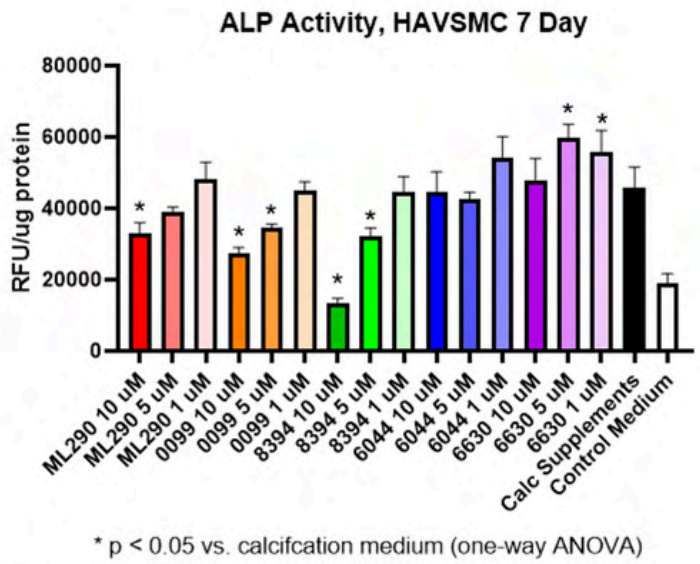

Fig. 1 Alkaline Phosphatase assay demonstrating the effect of multiple relaxin receptor agonists.

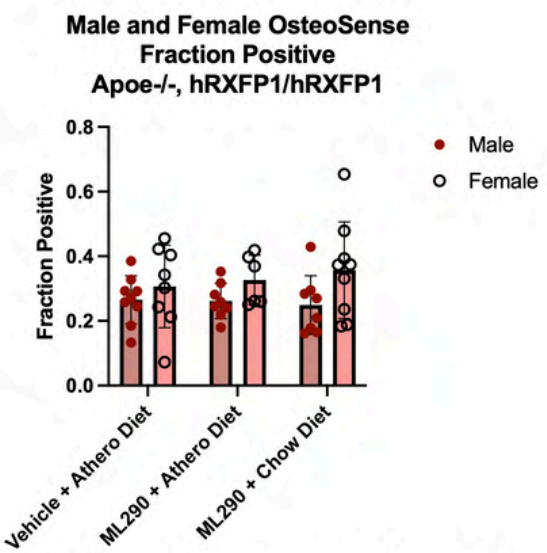

Fig. 2 Quantification of calcium probe, OsteoSense, in mice aorta treated with relaxin receptor agonist ML290.

Tissue Curvature Correction using Monte Carlo Simulation for NIRS Imaging

Authors: Himaddri Shakhar Roy, Kacie Kaile, Fernando Sebastian Chiwo, Daniela Leizaola, and Anuradha Godavarty

Faculty Advisor: Dr. Anuradha Godavarty

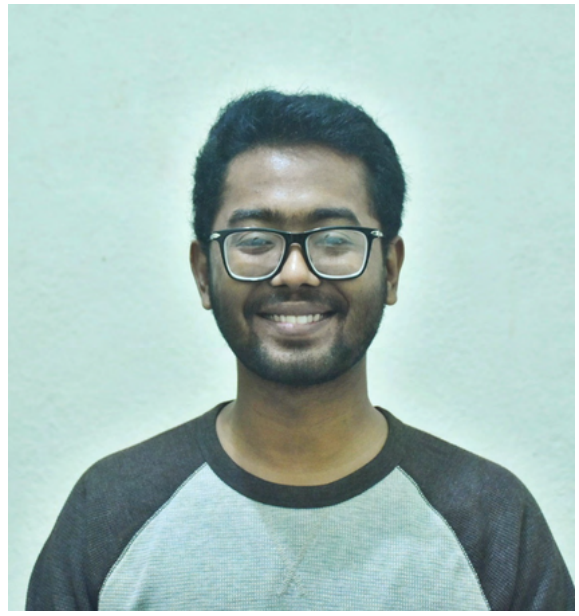

Diabetic Foot Ulcers (DFUs) causes serious risks to patients with diabetes which includes infections, amputations, and potentially death. Tissue oxygenation promotes the cellular formation of tissue and very crucial for wound healing. To assess the healing progress of DFUs, optical imaging techniques are being widely used to measure tissue oxygenation within the wounds. However, optical detector captures signals from focused flat-plane surfaces and DFU are often curved, particularly in cases of foot amputation. This curvature can distort tissue oxygenation measurements, leading to inaccurate assessment of the wounds. The tissue oxygenation measurement can be affected by the tissue physiology or tissue curvature. Therefore, it is crucial to remove the effect of tissue curvature to accurately measure tissue oxygenation changes in DFUs. In this study, the objective is to address irregular curved geometries and develop a correction model using Monte Carlo simulated diffuse reflected signal measurements. Two different tissue models (Fig. 1) have been simulated mimicking deep and protruded tissue and the simulation was run with uniform and gaussian light source. By applying height and angle corrections to the diffuse reflectance signals, we found that the correction factor improves the signal and reduce errors up to 11 % caused by differences in wound depth and surface angle. Our ongoing research focuses on implementing this correction factor for irregular curved geometries and determining the threshold for depth and angle corrections requiring correction when imaging curved tissue geometries.

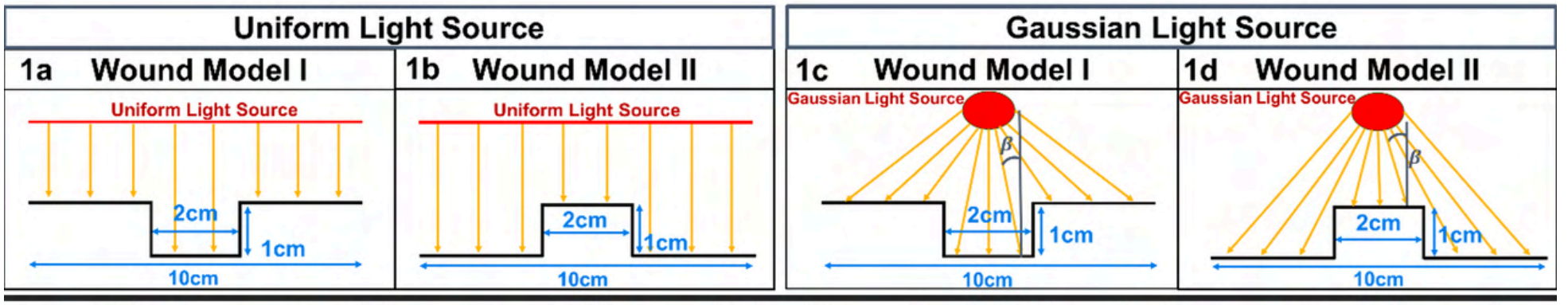

Fig. 1 Simple geometry of the wound model I (1a and 1c) and wound model II (1b and 1d). The red line indicates the Uniform Light Source and the red circle (1cm diameter) indicates the Gaussian light source. The orange arrows show the light illumination on the wound surfaces and β is the angle between the vectors of light illumination and surface normal.

Development and Characterization of Designed Electrospun Nanofibers for Cardiac Patch

Authors: Alexi Switz, Anamika Prasad, and Darryl Dickerson

Faculty Advisors: Dr. Anamika Prasad and Dr. Darryl Dickerson

Structure and fiber orientation dictate the hierarchical structure of biological materials and impact their mechanical and physiological outcome. Structures with coiled fibers, for example, promote elasticity and flexibility, whereas those with aligned structures promote higher strength. Helically coiled nanofibers are suitable for cardiac applications due to their inherent elasticity in a dynamic environment, along with other functionality such as hydrophobicity and large surface area for biomolecular interactions. While directed fibers are the hallmark of biological systems, replicating and controlling fibrous structures, specifically helically coiled fibrous structure, in engineered systems is challenging. We focused on using electrospinning as a manufacturing platform to produce and characterize directed fiber mats. Through this work, our key contribution is towards the development of electrospinning as a reliable, reproducible manufacturing method as well as establishing its significance and relevance in designing electrospun fibers for tissue engineering applications. We developed a manufacturing method using an affordable in-house electrospinning platform to create aligned, helically coiled and random fibrous mats for cardiovascular tissue engineering applications (Figure 1). We used a bioink comprised of polycaprolactone and dichloromethane as our polymer solution. Polycaprolactone is biocompatible and biodegradable, making it a suitable polymer for tissue engineering applications. Testing was conducted on the fibers to evaluate their mechanical properties and physiological outcome. Fiber structure was characterized using scanning electron microscopy and post-processed using ImageJ software. The composition of the fibers was assessed using Raman spectroscopy. The mechanical response was characterized via tensile testing (Figure 2). Limited tests were performed to evaluate the fiber's biocompatibility and capability to support cardiomyocyte activity. Imaging showed the in-house electrospinning platform and associated parameters resulted in reliable, replicable and accurate production of aligned and helically coiled fibers. Testing data showed promising results for fibrous mats applications in the development of a cardiac patch to treat deceased tissue resulting from a myocardial infarction

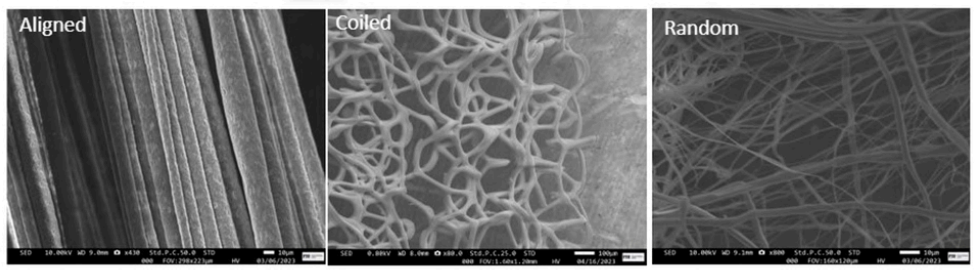

Fig. 1- SEM Images of aligned, helically coiled and random fiber mats made of PCL and DCM solution.

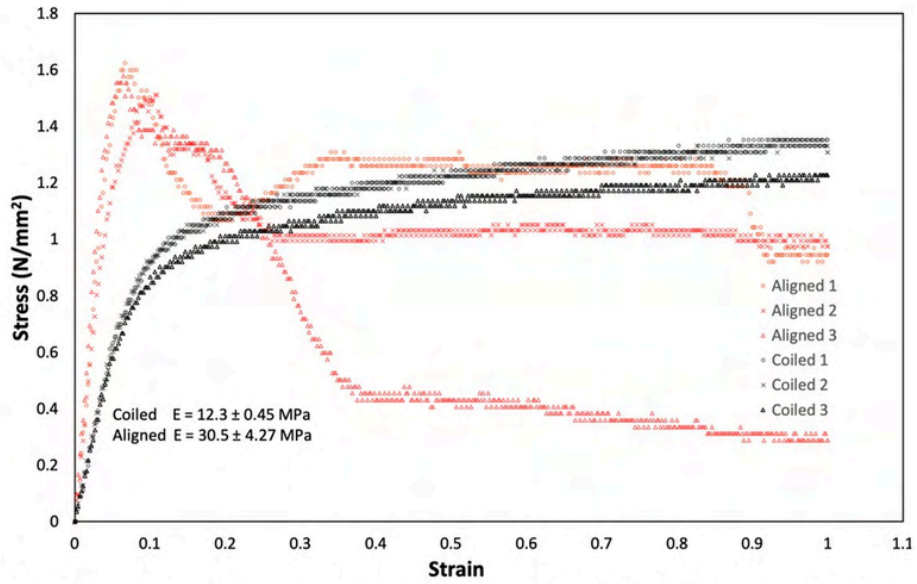

Fig. 2 -Tensile testing of aligned and coiled fibers under 100% displacement (CellScale Tensile Tester)

Human-in-the-Loop iBCI Model and monkey Validation of a Discrete Decoder

Authors: Pedro Alcolea and Zachary Danziger

Faculty Advisor: Dr. Zachary Danziger

Constructing effective new neural decoding algorithms for invasive brain-computer interfaces (iBCIs) is challenging because so few human test subjects are available and offline testing is not predictive closed-loop performance. Here we introduce and validate the direction selection (DS) decoder. DS maps neural firing into a selection off a small menu of preset velocities to operate a computer cursor, breaking with conventional strategies of mapping into a continuous 2D velocity field. With 48 naïve able-bodied human subjects using a closed-loop iBCI model over multiple visits, we compare DS against three common velocity field decoders: assisted direct regression (DR-A), ReFIT, and velocity Kalman Filter (vKF). DS outperforms DR-A, ReFIT, and vKF by a substantial margin (93%, 56%, 39%, and 26% of targets hit). We further demonstrate that a monkey subject using DS in an iBCI cursor control task substantially outperforms a DR-like velocity field decoder. The success of DS in both the online iBCI model and monkey comes despite its inability to closely reconstruct calibration trajectories offline, highlighting the importance of closed-loop evaluation and human-in-the-loop iBCI models.

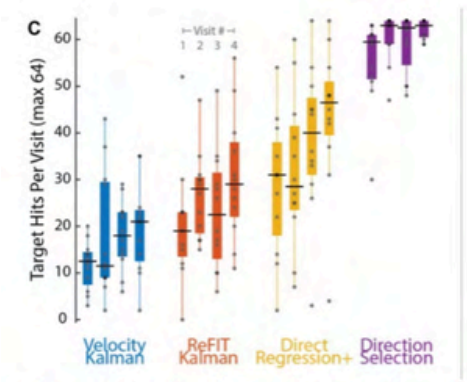

Figure 1: Boxplots of number of targets hit in the center-out task, outer grouping by decoder used (color) and inner grouping by visit number. Performance increases with repeated visits (learning) and decoder used significantly affects performance. Dots are individual subjects (some overlap), black bars are the median, solid box is the interquartile range, and whiskers extend to the most extreme points that are within 1.5 s.d. ± the mean. Data is aquired from 48 human subjects.

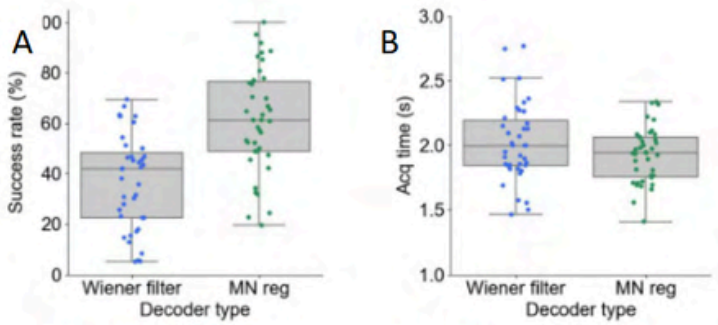

Figure 2: A) Each dot represents the percent success rate of either the Wiener filter or the DS decoder. The boxplot is as described in figure 1. B) Similar to A, however this time the Y axis is describing the average amount of time the monkey took to reach the targets per trial. Data is acquired from a Macaque, that uses each decoder at different times.

The Neural Recruitment of Executive Function in Monolingual and Bilingual Preterm Born Children

Authors: Noble Amadi and Wei-Chiang Lin

Faculty Advisor: Dr. Wei-Chiang Lin

Children born preterm are greater risk for deficiencies in executive functioning (EF) as compared to term-born children. While bilingualism has been shown to enhance the EF of term-born children it has yet to be explored whether bilingualism also enhances the EF of preterm-born children. This research explores the influence of bilingualism on executive function (EF), particularly focusing on inhibitory control, in preterm-born children. The study focuses on comparing inhibitory control, a crucial aspect of executive functioning (EF), in monolingual and bilingual preterm-born children. We employ the Go/No-Go (GNG) task, a recognized tool for evaluating inhibitory control, alongside functional near-infrared spectroscopy (fNIRS) to assess cerebral responses, thus enabling a comprehensive comparison of EF in both groups. We analyzed brain activity and compared inhibitory control in 23 preterm-born children, aged 6-7 years, who were categorized as either monolingual or bilingual based on detailed language assessments. Our findings reveal that in the GNG task, bilingual children exhibited a significantly faster response time while maintaining comparable accuracy to their monolingual counterparts. Additionally, the fNIRS data indicates that in the same Brodmann-Areas (BA) typically activated during Go/No-Go (GNG) tests, bilingual children show a weaker oxygenated hemoglobin ([HbO]) response compared to monolingual children, suggesting a more efficient neural engagement in executive function (EF).These results underscore the potential cognitive benefits of bilingualism in enhancing inhibitory control among preterm-born children, highlighting its importance in early educational and clinical strategies aimed at mitigating EF deficits associated with prematurity.

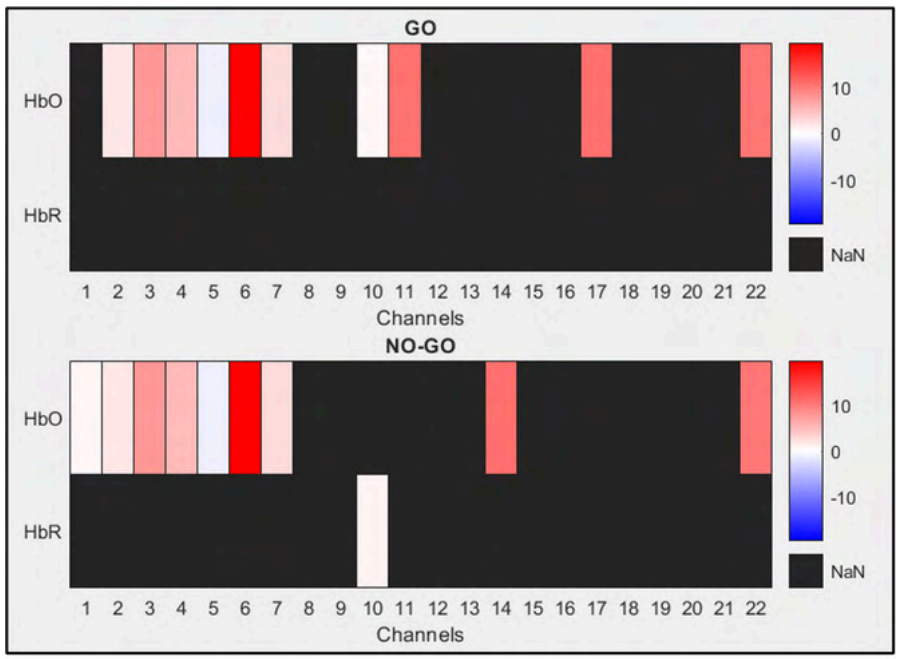

Fig.1 Figure Showing the Between - Group Analysis $[\beta_{mono} - \beta_{bi}]$

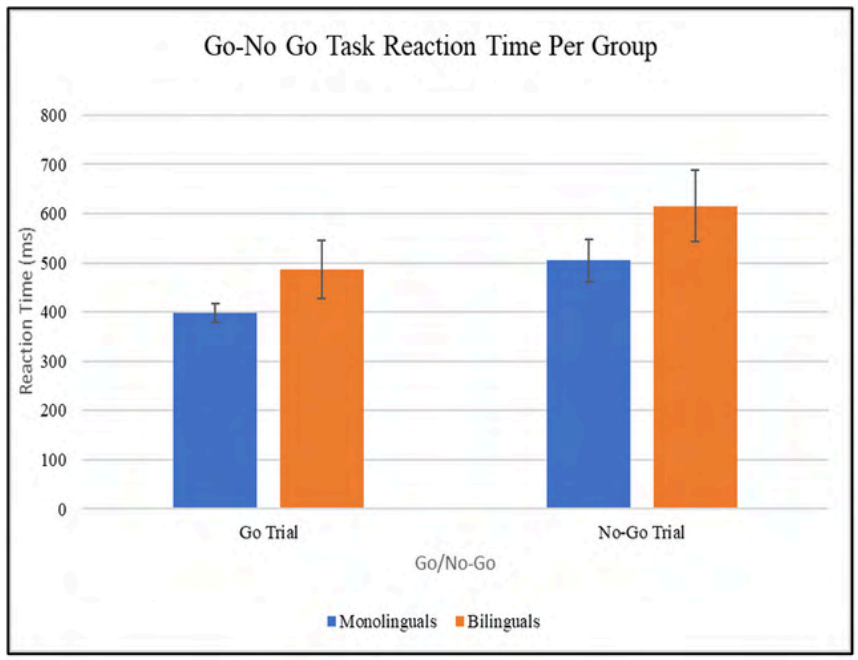

Fig.2 GNG Reaction Time for Bilinguals vs. Monolinguals.

The Effect of Robot Variables Controlled (Joint Angles/End Effector Position and Orientation) on Operator Skill Acquisition in High-Dimensional Hand Control of a Robot Arm

Authors: Steafan Khan and Zachary Danziger

Faculty Advisor: Dr. Zachary Danziger

The best way to give people control over complex robots (e.g., surgical robots, excavators, or mobile industrial robots) remains an open question. In this work we explore the possibility of turning a user's finger joint angles into a high-dimensional "joystick", letting us harness a fluid and rich space of user signals for robot control (Fig 1.). This, however, raises the question of what robot variables we should map the user's hand into. Previous studies, investigating control of computer cursors, found that people's performance at cursor control tasks is substantially impacted by the cursor variables that they control (e.g., cursor position versus velocity). We hypothesize that the effect of variables controlled has an even greater impact when controlling robots due to the added dynamics. In this work, we provide two groups of n=4 healthy participants control of a 6 DOF robot via the 19 joint angles of their fingers. Participants in each group are provided control over a different set of robot variables: robot joint angles, or robot end effector position and orientation. To map the user's input into robot commands we linearly project (via subject-calibrated Principal Components) the 19-D finger joint angles to the 6-D robot commands. Participants in both groups control the robot to perform the same task of picking up objects and placing them into target locations. Participants are evaluated in terms of the time it takes them to complete each task stage (where stages are gripper contact with object -> object grasp -> object lift -> object place). We find that participant performance is highly varied across our groups with some participants becoming skilled while others remain unskilled at the task (Fig 2.). The large inter-participant variability dominates any effect of the robot variables controlled on operator skill. We also find that participants' performance early on is highly predictive of their acquired skill at the end of practice across our groups. Our results suggest that, regardless of robot variables controlled, large improvements in operator skill acquisition may be obtained through individual specific interventions like varying feedback or adapting the robot-user-interface.

Fig 1. *Photo of the experiment setup. The 6 DOF robotic arm (left) is being piloted by the participant (right) wearing a CyberGlove.*

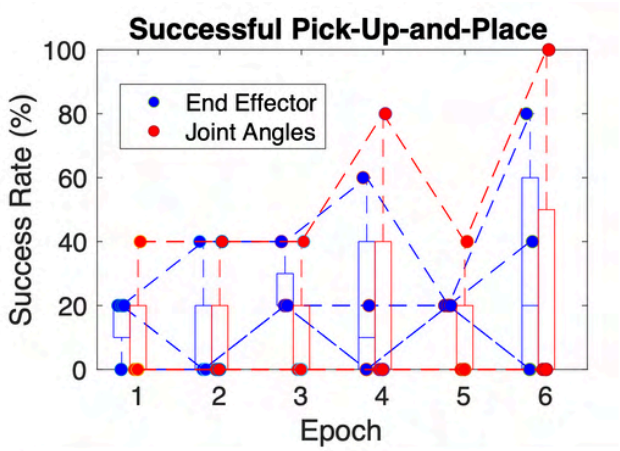

Fig 2. *Participants' percentage of successful trials per experiment epoch (5 trials). In both groups there is large inter-participant variability which dominates any effect of robot variables controlled.*

An objective aid for diabetic foot ulcer debridement utilizing an in-house NIRS imaging device

Authors: Daniela Leizaola, Kacie Kaile, Maria Hernandez Hernandez, Renato Sousa, Jose Ponce, Stanley Mathis, Alexander Trinidad, Nikhil Vedere, Himaddri Roy, Manuel Leizaola, David Armstrong, and Anuradha Godavarty

Faculty Advisor: Dr. Anuradha Godavarty

Diabetic foot ulcers (DFUs) are a significant challenge for diabetic patients and largely affect their lifestyle. Currently, clinical assessment of DFUs primarily relies on visual cues by the patient and/or clinician, which results in subjective evaluations. Scalpel debridement is a standard intervention to promote wound healing by removing non-viable tissue and enhancing the potential to heal. The quantity and location of tissue to remove remains a subjective assessment; thus, an objective method by optical imaging could improve the scalpel debridement process. To address this gap, an in-house noncontact near-infrared spectroscopic (NIRS) imaging device, named SPOT, was utilized to provide spatial (2-D) tissue oxygenation maps of DFUs during the debridement process.

Fifteen subjects were recruited and imaged across four weeks (40 cases) to evaluate tissue oxygenation changes before and after scalpel debridement using the SPOT device. SPOT captures diffuse reflectance signals at discrete near-infrared wavelengths (690, 810, 830nm) to reconstruct effective hemoglobin-based parameters (e.g. oxygen saturation) by applying a modified Beer-Lamberts law. Preliminary results (6 cases) revealed distinct increases in oxygen saturation (ΔStO2) in regions outside the wound (when compared to the wound) following debridement, shown in Fig 1. In turn, a reduction in the contrast between the two regions (more homogenous) post-debridement was prominent, seen by the percentages in Fig.1. On-going work involves analysis of all cases to determine the potential of using SPOT as an objective guide in debridement procedures by identifying regions that might still require removal

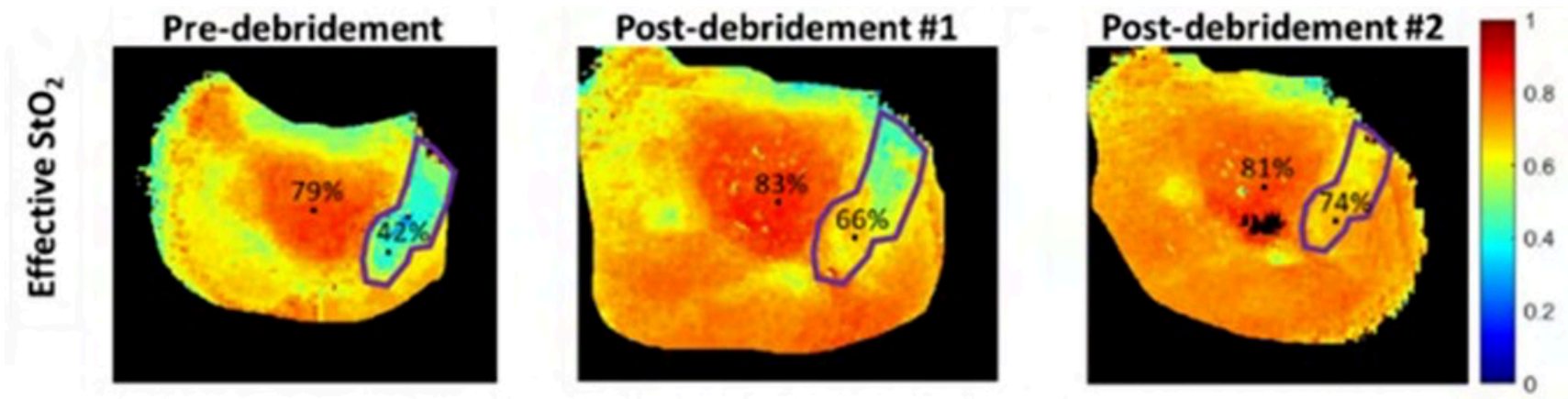

Fig 1: Effective oxygen saturation (ΔStO2) maps of a post-amputee DFU case pre- and post-debridement obtained using the SPOT device. Regions demarcated in purple on the ΔStO2 maps represent the callused tissue on the surrounding region of the wound that was used for quantitative analysis. The percentages represent the mean ΔStO2 values in the wound and the selected callused tissue region.

Developing an Algorithm for In-Vivo Detection and Feature Analysis of Sharp Wave Ripples in the Common Marmoset Hippocampus

Authors: Carlos Otero and Jorge Riera

Faculty Advisor: Dr. Jorge Riera

Sharp wave ripples (SWRs) are neurophysiological events observed in the hippocampus, characterized by a combination of a low-frequency (sharp wave) and several high-frequency oscillations (ripple). These events result from synchronized neural firing within the Cornu Ammonis (CA) of the hippocampus and have been linked to memory transfer and consolidation from hippocampus to other cortical areas of the brain. Although SWR are thought to be universal across species, most studies have been conducted using a rodent model. There is a need to conduct studies of SWRs in other species more similar to humans such as non-human primates. This could enhance the translational value of animal models and our capacity to understand human cortical circuits. However, challenges in detecting SWRs in primates include lack of studies, heterogeneity in electrode types, and noisy datasets. This study focused on developing a detection algorithm that analyzes LFP time series recordings (Low pass filtered at 300Hz) from a non-human primate, the common marmoset that has become a popular model for translational neuroscience. We design an algorithm to detect the sharp wave (1-10Hz) and ripple (150-250Hz) components and identify epochs where both components overlap and corroborated the results by visual inspection of the SWR morphology. The algorithm successfully detected classical SWRs within freely moving marmoset (Fig. 1) allowing for further feature analysis of these events. The analysis of these features— such as the duration, power, and mean frequency of the ripple and sharp wave components, correlation across channels during the events, as well as the coupling between the phase of the sharp wave and the amplitude of the ripple— provides insight into the characteristics of SWRs in primates. Moreover, it builds a database of SWRs in the common marmoset that can be used in the future for comparisons with other species.

Fig. 1: Various examples of in vivo marmoset SWRs detected with their ripple and sharp wave components.

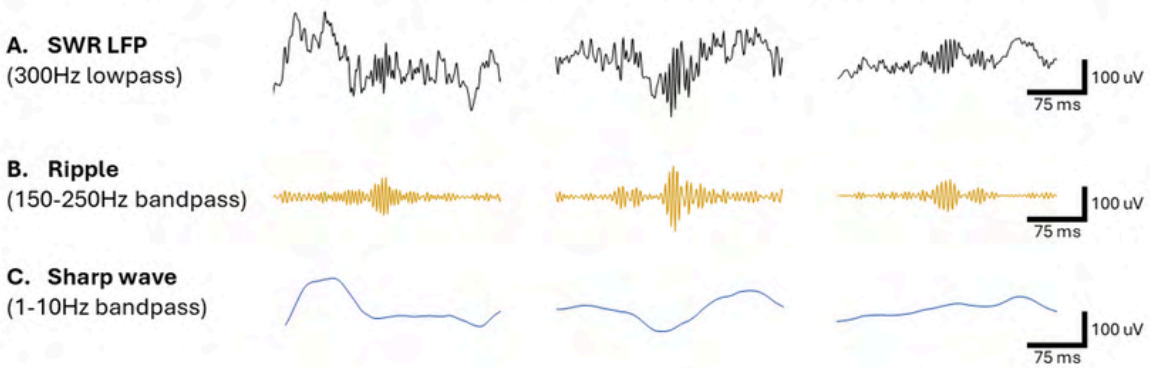

A This row depicts three different events detected within a marmoset in vivo recorded from a micro brush array and filtered to the LFP using a 300Hz lowpass filter. **B** Within this row the time series is filtered into the Ripple bandpass range of 150 – 250Hz range to show the high frequency oscillation of the SWR , each ripple is underneath its respective SWR LFP signal. **C** The last row displays the low frequency sharp wave bandpass range of each of three events between 1 – 10Hz. Each of the rows have scaled bars to represent the scale of the voltage and time of the signal which is the same for the three rows.

Beyond the Barrier: Assessing Drug Penetration in a Brain Tumor Model with an Integrated Blood-Brain Tumor Barrier

Authors: Umme Hafsa Momy and Anthony McGoron
Faculty Advisor: Dr. Anthony McGoron

This research tackles a critical challenge in brain tumor treatment: delivering drugs across the blood-brain barrier (BBB). The BBB acts as a protective shield for the brain, but it also blocks many medications from reaching brain tumors. Our innovative approach involves engineering 3D models of the blood-brain tumor barrier (BBTB) using spheroids—tiny, organ-like structures composed of cancer, brain, and endothelial cells. So far, our team has constructed spheroids from astrocytes and neuroblastoma cells to form initial models of brain tumor tissue. We've prepared various environments for these spheroids to grow, aiming to simulate the BBTB as closely as possible. The next step is to create complex co-cultures by adding brain endothelial cells, which are essential to the BBB. The goal is to develop an integrated BBTB spheroid model that also incorporates tumor associated macrophages and other immune cells composing the tumor microenvironment. This will help us to better understand how the BBB operates and its role in brain cancer progression and resistance to treatment. More importantly, it will allow us to test how well drugs can penetrate the BBB to reach brain tumors. Our work could significantly impact the development of more effective treatments for brain tumors, offering new hope to patients.

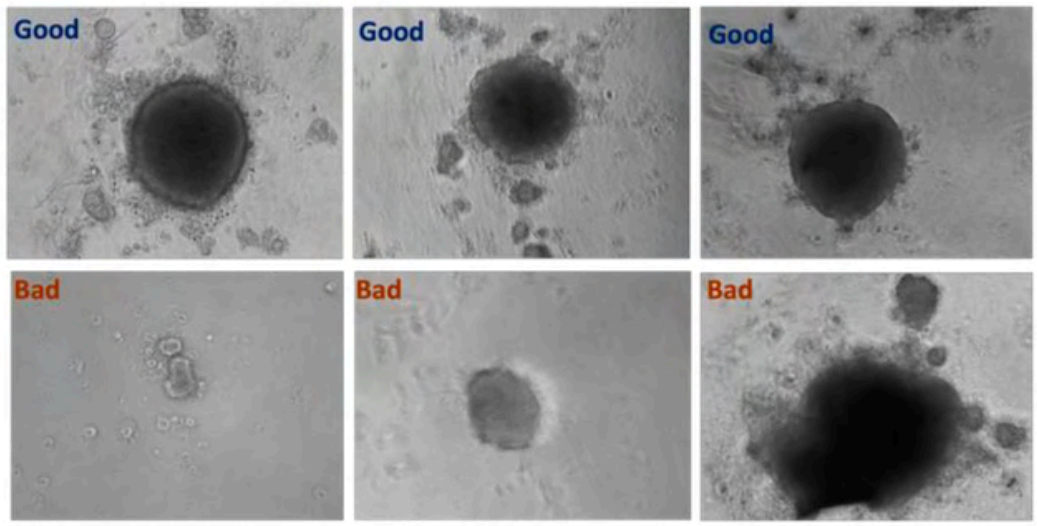

Fig.1: Shown Bright-field organoids, acceptable (good) vs. unacceptable (bad) quality assessment.

Dynamics and diurnal patterns of spontaneous, recurrent seizures in a mouse model of repetitive blast traumatic brain injury

Authors: Md Adil Arman and Oleksii Shandra

Faculty Advisor: Dr. Oleksii Shandra

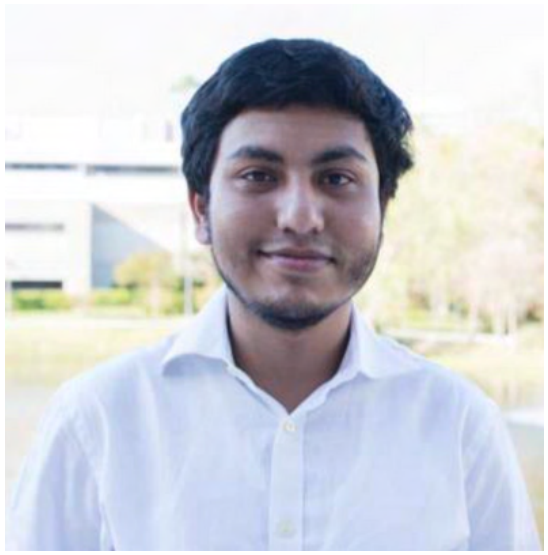

Introduction: In the last twenty years, approximately 500,000 members of the U.S. military have been affected by traumatic brain injury (TBI). One of the debilitating sequelae it carries is the development of post-traumatic epilepsy (PTE), indicated by spontaneous recurrent seizures that can arise from several months to years after an insult to the brain. The occurrence is substantially higher among military personnel, between 32% and 43%, compared to civilians, at rates ranging between 7% and 25%. Blast injuries due to improvised explosive devices (IEDs) are the leading cause of military TBI and account for approximately 60% of all military TBIs and up to 80% of mild TBI. In comparison with civilian TBIs, which for the most part result from accidents or falls, these present unique challenges and exhibit an increased incident rate. Adding more to the complexity and repetitiveness of the blast exposures, with a concomitant increased prevalence, are the long-term neurological complications that come with PTE. Here, we hypothesized that seizures after repetitive blast TBI have the diurnal patterns. Knowledge of the dynamics and patterns of post-blast-induced TBI is crucial in the identifying reliable biomarkers and for development prevention and effective treatment strategies.

Methodology: We used a mouse model of repetitive blast-induced TBI in male and female mice aged 12-16 weeks. Mice were anaesthetized and exposed to a controlled blast wave using the blast simulator, which produced primary blast injuries characterized by a peak static overpressure of approximately 117 kPa for a duration of 2.5 milliseconds.. For comparison, control animals were exposed to an audio stimulation only. To assess the impact of TBI, we monitored seizure onset and changes in the power spectrum through continuous video-EEG for four months post-injury.

Results: 11 out of 53 blast-injured mice developed PTE, with a higher incidence in females (25%) compared to males (19%) showed in Fig.1. Seizure frequency analysis, supported by a one-way ANOVA and Sidak's multiple comparisons test, revealed significant variability among animals ($p=0.0042$ and $p=0.0073$, respectively). Notably, seizure occurrences were three times more frequent during the light period compared to the dark period, suggesting a 200% increased seizure rate during the light period (Fig. 2). This finding indicates a potential link between the sleep-wake cycle and increased seizure susceptibility in blast-injured mice.

Discussion: Our study enhances the knowledge of PTE, following blast TBI and highlights significant diurnal variations of seizure occurrence. This further emphasizes the importance for consideration of the sleep-wake cycle in management and treatment of PTE, which might dictate therapeutic interventions for minimizing the risk of seizures.

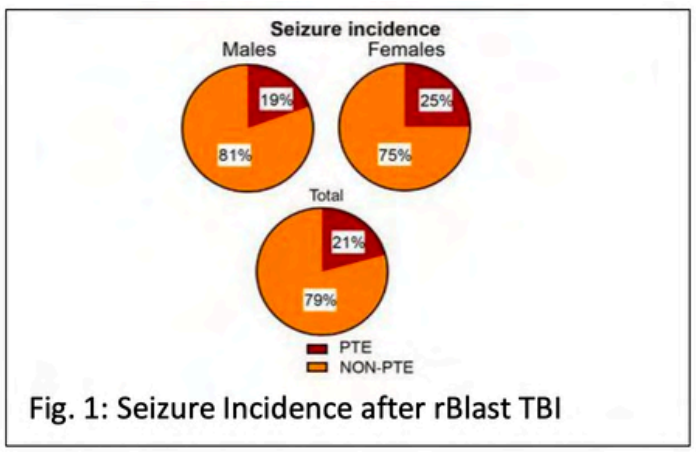

Fig. 1: Seizure Incidence after rBlast TBI

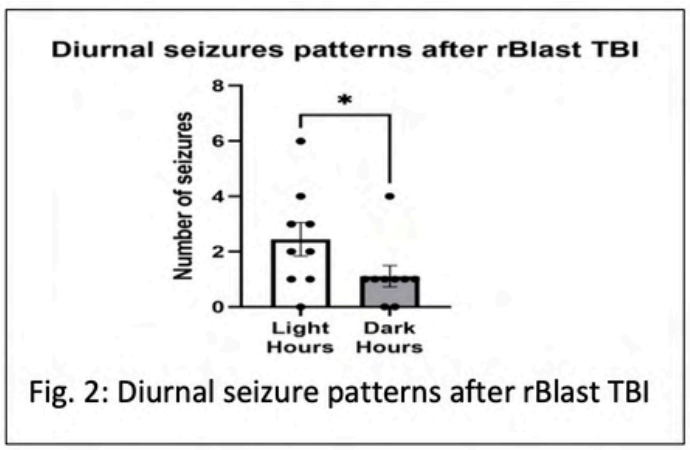

Fig. 2: Diurnal seizure patterns after rBlast TBI

Elucidating the Histochemical Response of Elastin-Rich Valves to Varied Levels of Natural and Inflammatory Cells

Authors: Claudia Ponce Aportela and Sharan Ramaswamy

Faculty Advisor: Dr. Sharan Ramaswamy

Significance: Valvular diseases, particularly as congenital heart valve defects, pose significant challenges in pediatric healthcare, necessitating valve replacements in children. Conventional therapies often prove inadequate, underscoring the urgency for novel solutions. This research explores the potential of tissue-engineered valves enriched with elastin to evolve and expand alongside patients. Through integrating allogeneic valves with extracellular matrix (ECM) components, the study seeks to examine their capacity to attract endogenous heart valve cells and facilitate bodily growth. This study seeks to explore this by conducting a test involving immune and native heart valve cell co-cultures, examining cytokine activation and ECM production, including muscle cell integration, elastin, collagen, and mucins generation.

Method/Approach: Tissue Engineered Elastin covered Porcine Small Intestinal Submucosa (PSIS) were co-cultured with human Valvular Endothelial Cells (hVECs) and human Valvular Interstitial Cells (hVICs) in co-culture for 8 days under rotisserie conditions. The culture medium conditions were Dulbecco's Modified Eagle Serum (DMEM), 2% Penicillin/Streptomycin, 10% Fetal Bovine Serum (FBS), Ascorbic Acid and lastly, basic fibroblast growth factor (bFGF). Following initial seeding, the samples were further co-cultured with M0 macrophages, which are known for their non-activated polarization, to evaluate the immune response and determine the polarization towards M1 (pro-inflammatory) or M2 (anti-inflammatory) upon exposure to the natural cell environment. The recuperated media was then centrifuged at 1500 RPM for 15 minutes with the purpose of removing the debris and stored at -800C. Control samples, consisting of non-tissue-engineered PSIS, underwent the same co-culture process for comparative purposes. All samples were preserved in Optimal Cutting Temperature (OCT), frozen at -80°C, sectioned at 16µm thickness, and stained using Movat's Pentachrome. The analysis of the culture media was conducted using a custom ELISA cytokine panel to detect a range of pro-inflammatory and anti-inflammatory markers.

Major observations/Results: Findings demonstrate an increased ECM components for tissue engineered elastin valves with a statistical difference ($p \leq 0.05$) on all samples. There is a significant difference in the expression of specific proteins between the two valve types. The tissue engineered elastin rich valve exhibited a higher expression of elastin, Fibrin_Muscle/Nuclei, Collagen and Mucins Figure 1. The cytokine analysis revealed elevated levels of expression in the elastin-enriched covered valves compared to the untreated PSIS scaffolds; however, these differences were not statistically significant, as shown in Figure 2. Among the evaluated cytokines, IL-6—which is indicative of acute phase inflammation and fibrinogen production—was the only one observed to have higher expression levels in the untreated PSIS scaffolds. Statistically significant differences were noted for IL-8 and IGF-1 ($p \leq 0.05$), which are associated with tissue chemotaxis (the recruitment of nearby cells) and the promotion of tissue valve growth and repair, respectively. This experiment, therefore, demonstrates, from an in-vitro perspective, the advantages of an elastin-rich valves.

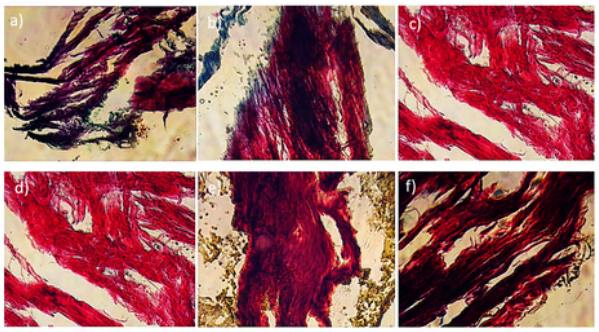

Fig.1 Raw PSIS Scaffolds (a-c) ECM secretion quantification in comparison to Engineered Elastin Rich Valves(d-f) after 16-days static rotisserie co-culture with hVICs, hVECs and, Macrophages, (n = 2 specimens/group, sectioned at 16 µm from the outer surface). collagen(yellow/orange), fibrin or muscle(red), mucins (blue/green) and elastin (purple/black), Magnification 10x.

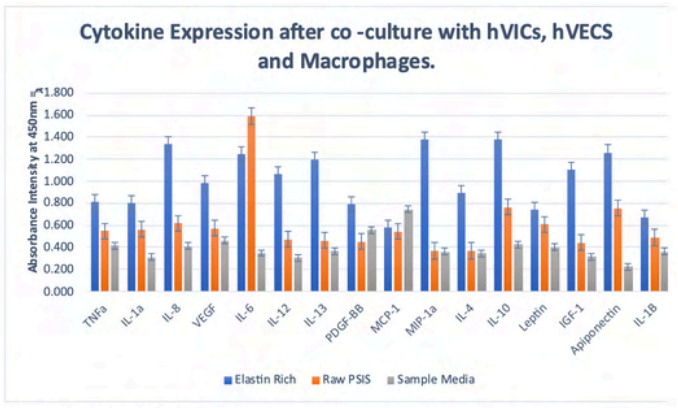

Fig. 2 Comparison of Cytokine Absorption Intensity in two Independent Samples of Tissue Engineered Elastin Rich and Raw PSIS Culture Media After a 16-Day Period of Static Rotisserie Incubation.

Predicting Nitric Oxide Biotrasport in Microvascular Networks Using the Green's Function Method

Authors: Mahsa Saadat and Nikolaos Tsoukias

Faculty Advisor: Dr. Nikolaos Tsoukias

Nitric oxide (NO) plays a pivotal role in a variety of physiological processes, including in regulating blood flow and pressure. NO is produced by the endothelium and diffuses to the smooth muscle, initiating the process of relaxation. The NO production is dependent on Calcium (Ca2+) and involves transient bursts of NO/Ca2+ within the endothelial cells. Mathematical models have been examined NO production and transport around blood vessel identifying diffusional barriers that can modulate NO levels and reducing NO scavenging by RBCs. Here, a computational approach is presented to describe NO release and transport in three-dimensional microvascular networks based on the Green's Function. This method efficiently accounts for NO release by endothelial cells and consumption by Red Blood Cells (RBCs) flowing in complex vascular network geometries. Integration of the proposed approach with detailed models of blood flow in brain will provide a quantitative framework to elucidate mechanisms of blood flow control in health and their dysregulation in pathological conditions.

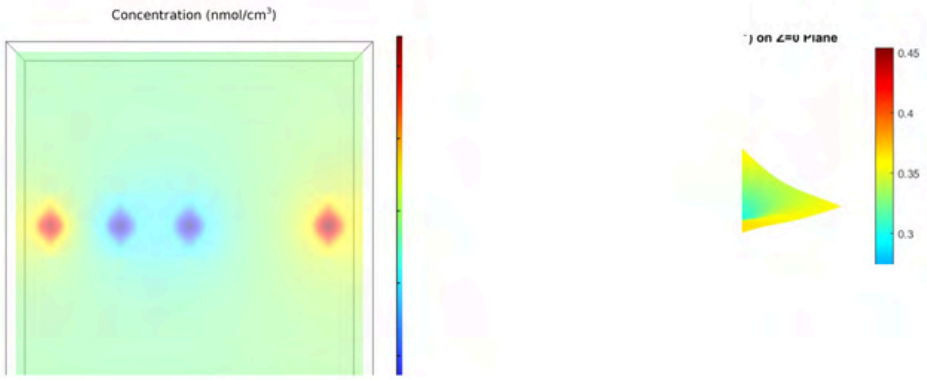

Fig. 1. Validation of Green's function Method against FEM simulations. Two NO production and two consumption points within a square domain

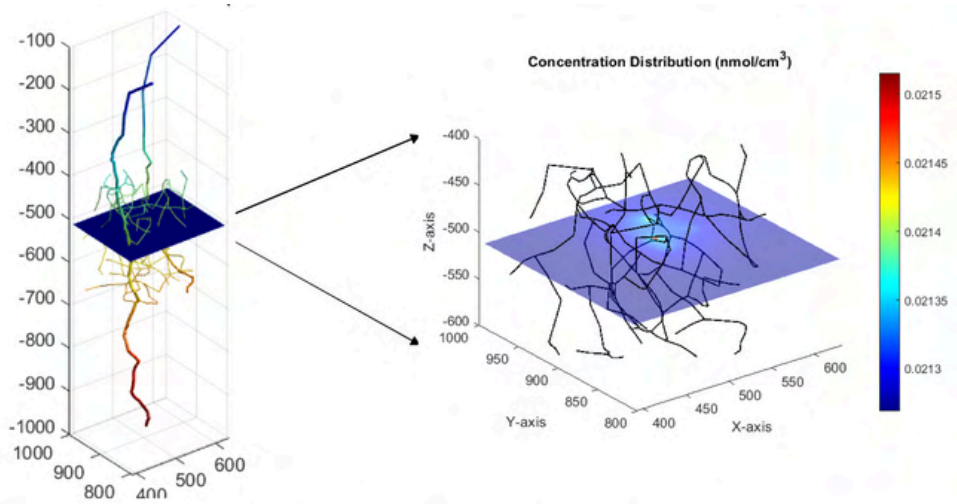

Fig. 2 NO release by brain capillaries

Augmented Data Glove for jaBCI

Authors: Peeyush Awasthi and Markondeya Raj Pulugurtha

Faculty Advisor: Dr. Markondeya Raj Pulugurtha

Our previous jaBCI (joint angle Brain Computer Interface) studies relied on Cyber Glove 3 systems as Data Gloves. These gloves, equipped with 19 sensors (highlighted yellow in Figure 1), captured finger kinematics based on joint movement. While the sensors provided accurate joint angle measurements (down to a degree or 0.01753 radians), they couldn't capture subject-specific finger features. To address this limitation and leverage the high dimensionality of the human hand (27 degrees of freedom controlled by 34 muscles), we explored using hand postures for jaBCI control (various postures shown in Figure 1a).

We developed an improved jaBCI solution for hand postures using micro-sized patch antennas resonating at 94 GHz, which could be mounted on finger joints (Figure 1b). Patch antennas were chosen due to their suitability for easier wireless telemetry to provide untethered user interfaces. Their miniature size at 94 GHz makes them highly sensitive to changes in surface curvature, essentially acting as aerial sensors for joint angles and finger structure. These antennas not only measure joint angles with a superior resolution of ¼ degree (0.00436 radians) but also account for finger curvature, a subject-specific feature. The resonant frequency of the patch antenna varies with joint angle resolution between 10 and 20 degrees. The curvature dependence was modeled using SolidWorks and simulated with Ansys HFSS. The joint angles are indirectly measured through the frequency deviation of the resonant peak, which occurs due to changes in the antenna's overall electrical properties caused by curvature variations. This augmented Data Glove can be used to generate highly personalized signals useful not only to Brain Computer Interface research but also to multiple application like augmented reality of real time control of complex features in any other domain.

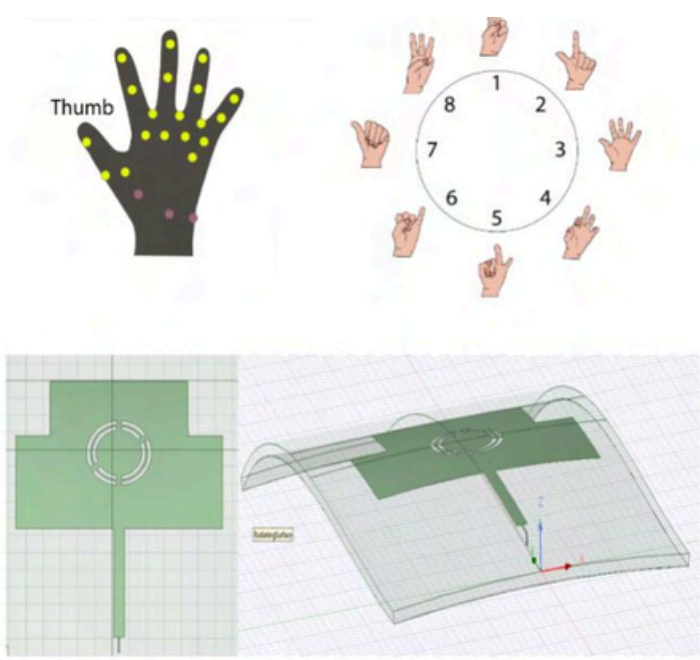

Figure 1: (Top) Sensors on data glove with postures used in jaBCI (joint angle Brain Computer Interface) model. (Bottom) Patch antenna (Aerial Sensor) - Top view and after bending on finger joints

Multimodal Sensing with Embedded-Electronic Flex Fan-Out Packaging

Authors: Reshmi Banerjee and Markondeya Raj Pulugurtha

Faculty Advisor: Dr. Markondeya Raj Pulugurtha

There is an imminent need to develop wearable or minimally-invasive implantable multimodal sensing systems, combined with AI (Artificial Intelligence) and ML (Machine Learning), to provide a unique combination of biomarkers. These should further stratify the outcome based on a new set of disease classifiers for accurate and autonomous continuous outcome predictors. Sensor fusion and reliable seamless wireless connectivity with external electronic readers through simplified circuit topologies, advanced telemetry components and 3D package integration are identified as the main barriers towards this technology. The primary focus of this is to develop a new class of embedded-component flexible fan-out packages with RF harvesting or inductive telemetry, embedded photonic devices in flexible packages, and wireless telemetry. Embedding allows integration of additional components into smaller volumes thus allowing vertical three-dimensional integration of multilayer packages with power harvesting. The strategy essentially consists of two parts: simplified circuit topologies for efficient power and data telemetry, and 3D package integration of sensor-communication chain for meeting the system targets. The key fundamental building block advances are demonstrated through in vitro testing from phantom tissue models. This research will lead to the miniaturized biophotonic patches, and thinnest and smallest EMG patches that operate at low interrogation power.

Biophotonic sensor prototypes are developed with embedded-chip technology, with both embedded light sources (LEDs) as well asphotodetectors in the flex package that provides a flat surface for the device-skin interface. This allows intimate contact of the photonic components with the skin and a large signal to noise ratio to allow detection at lower LED and detector power. Embedding of chips in flexible carriers was accomplished with direct screen-printed interconnects onto the chip pads in substrate cavities. Silver nanoflake-loaded polyurethane is utilized in the embedded-chip packages to provide the desired lower interconnect resistance and also reliability in flexible packages under deformed configurations. Various functional blocks of the prototype are currently fabricated and tested.

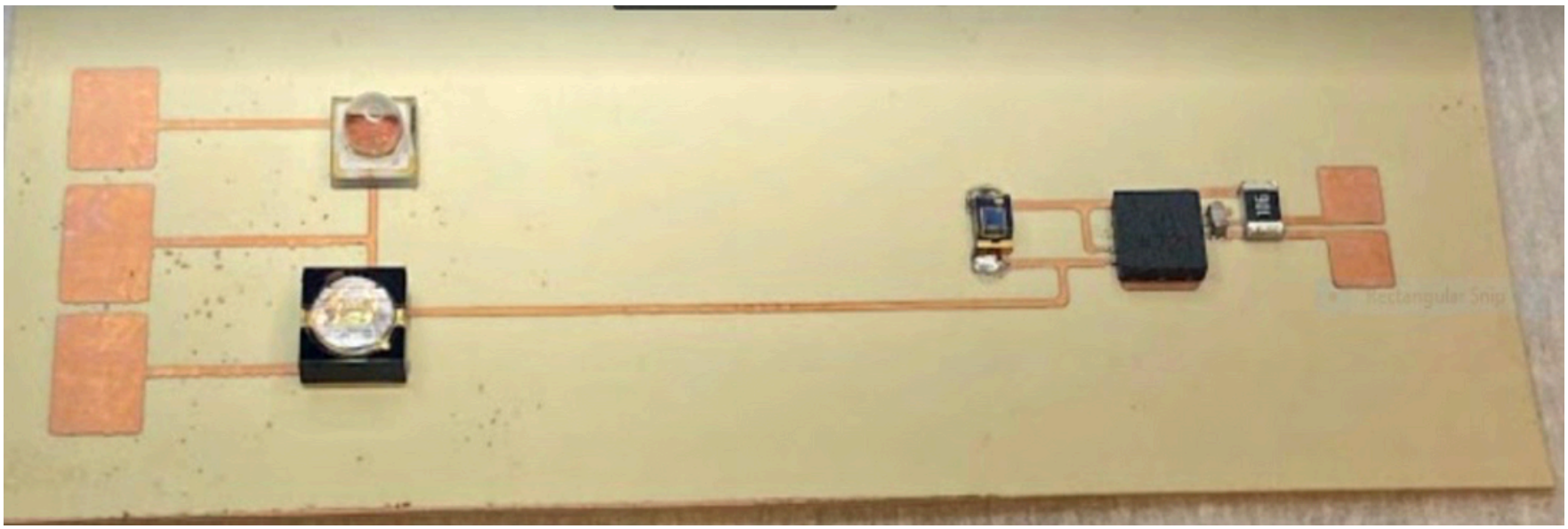

Development and Evaluation of a 3D Hydrogel-Based In Vitro Tumor Microenvironment Model for Drug Delivery Optimization

Authors: Jelena Obradovic and Anthony McGoron

Faculty Advisor: Dr. Anthony McGoron

Cancer is one of the main causes of death globally. Traditional treatments often damage normal tissues, as they do not discriminate between normal and tumor cells. Nanoparticle-based drug delivery systems can offer advantages such as accurate targeting of tumor cells, reduced side effects, and optimal pharmacokinetics. A significant challenge in nanoparticle-based treatment is the limited particle concentration that reaches tumor cells due to the complex microenvironment of the tumor. The majority of nanoparticles become trapped in the extracellular matrix (ECM) or are absorbed by tumor-associated macrophages. Nanoparticles mostly accumulate in the perivascular region and are not able to diffuse deeper into the tumor tissue, which limits their efficacy.

This project aims to explore how the tumor microenvironment impacts particle diffusion using a 3D hydrogel model that stimulates native ECM. The methodology will involve developing a 3D hydrogel model simulating the tumor ECM and measurement of the diffusion rates of various fluorescent drugs, polymers, and nanoparticles through the ECM mimic. In doing so, we aim to understand in what manner ECM structure influences transport and identify potential obstacles that need to be overcome for effective drug delivery. Additionally, various cells of the tumor microenvironment will be integrated into the model, investigating their influence on drug transport within the ECM. Ultimately, our goal is to contribute to the advancement of cancer treatment strategies by broadening the understanding of drug delivery.

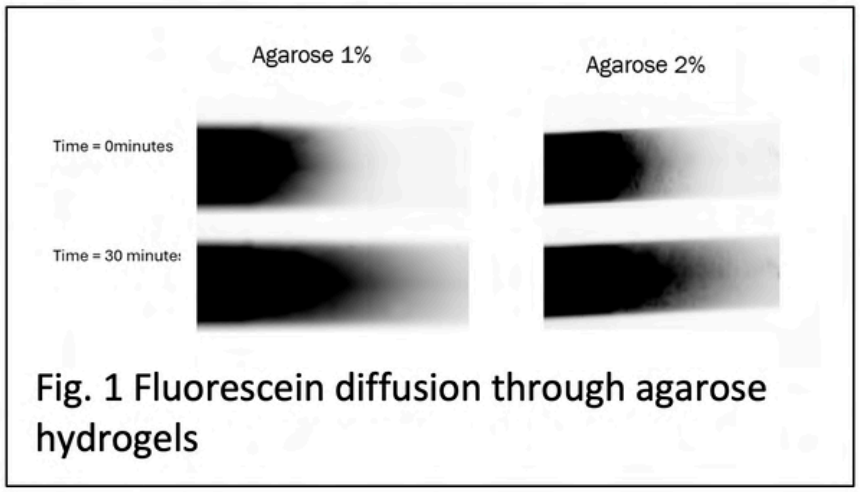

Fig. 1 Fluorescein diffusion through agarose hydrogels

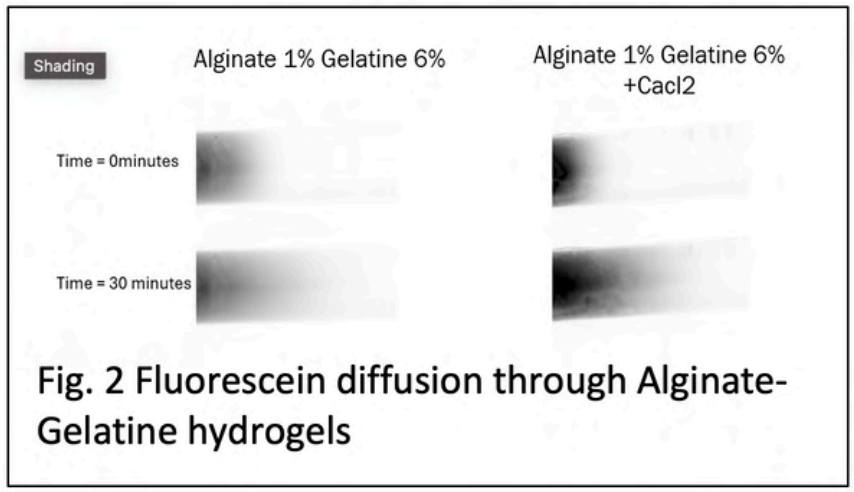

Fig. 2 Fluorescein diffusion through Alginate-Gelatine hydrogels

ABOUT OUR PROGRAM AND COLLEGE

The Department of Biomedical Engineering at Florida International University (FIU) located in Miami is committed to preparing ambitious students who want to combine their love of problem-solving with their desire to help others, through this fascinating growing field that applies cutting-edge technologies and modern engineering techniques to improve healthcare.

Our College of Engineering and Computing is ranked #1 for bachelor's degrees awarded to Hispanics, #1 for Bachelor's degrees awarded to Underrepresented minorities by total, #2 for master's degrees awarded to underrepresented minorities by total, and #56 among graduate programs in the country*. Nationally, we are among the Top 30 to award undergraduate degrees and Top 80 for research expenditures*. Florida International University is designated a Carnegie Highest Research (R1) and Carnegie Community Engaged Institution.

*US News 2023 *ASEE 2022 and NSF HERD 2019-2021

DREAM, DISCOVER,
INSPIRE, INVIGORATE

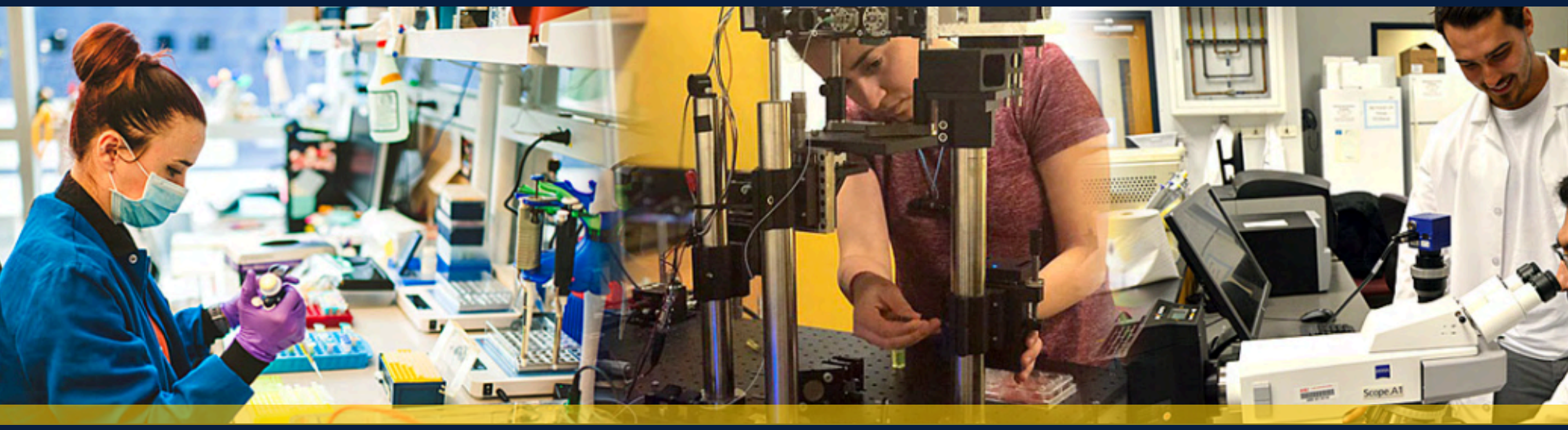

FIU | Engineering & Computing

Department of Biomedical Engineering

The Department of Biomedical Engineering at Florida International University (FIU) located in Miami is committed to preparing ambitious students who want to combine their love of problem-solving with their desire to help others through this fascinating growing field that applies cutting-edge technologies and modern engineering techniques to improve healthcare.

bme.fiu.edu

Presented through the generous support of the Wallace H. Coulter Foundation

Florida International University | College of Engineering and Computing

Department of Biomedical Engineering

10555 West Flagler Street Suite EC 2600 Miami, FL 33174